Crustal stress-state of Mongolian Altai by set of data

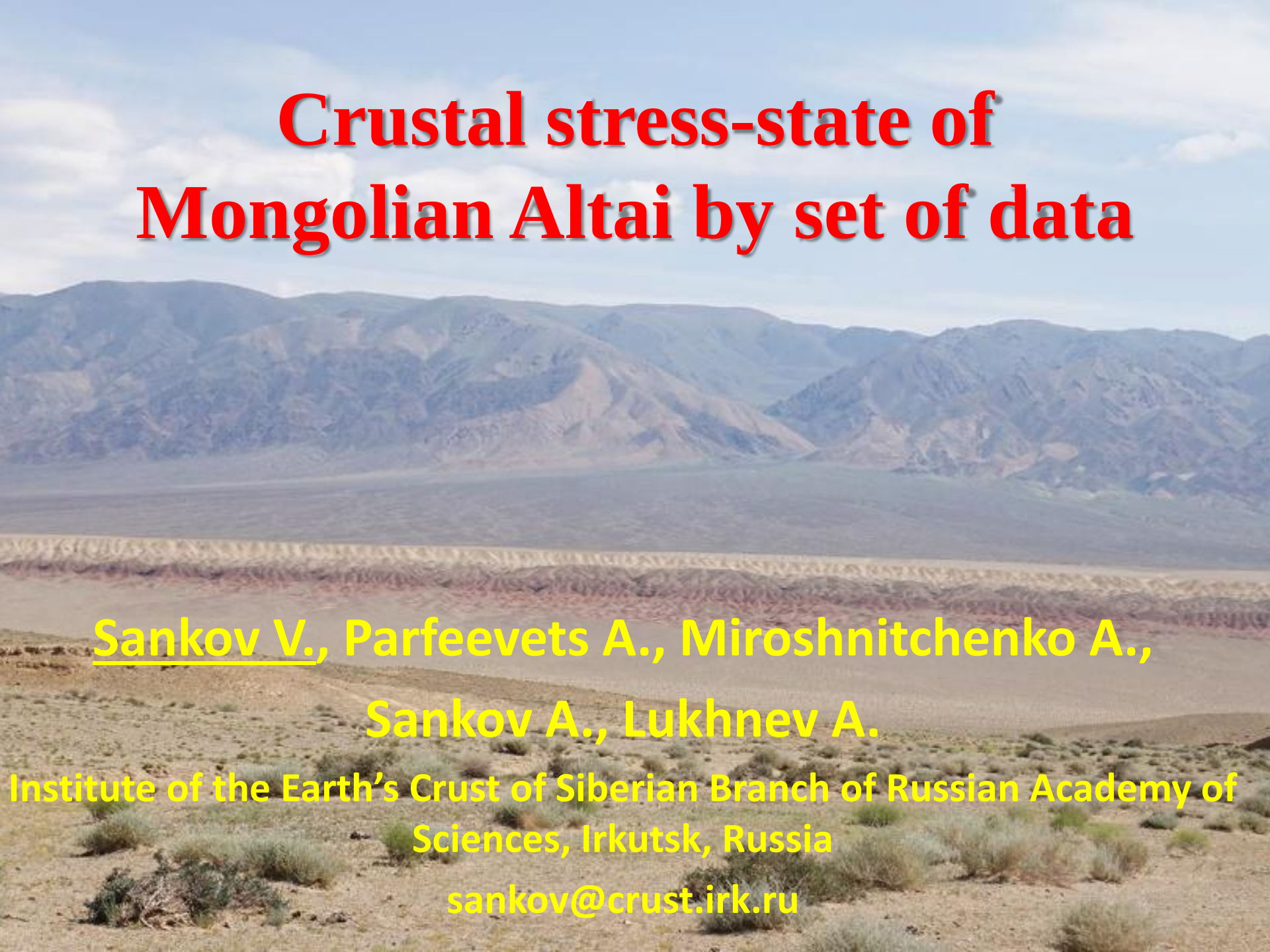

Sankov V., Parfeevets A., Miroshnitchenko A., Sankov A., Lukhnev A.

Institute of the Earth's Crust of Siberian Branch of Russian Academy of Sciences, Irkutsk, Russia

sankov@crust.irk.ru

Relief and Cenozoic active faults of Mongolia

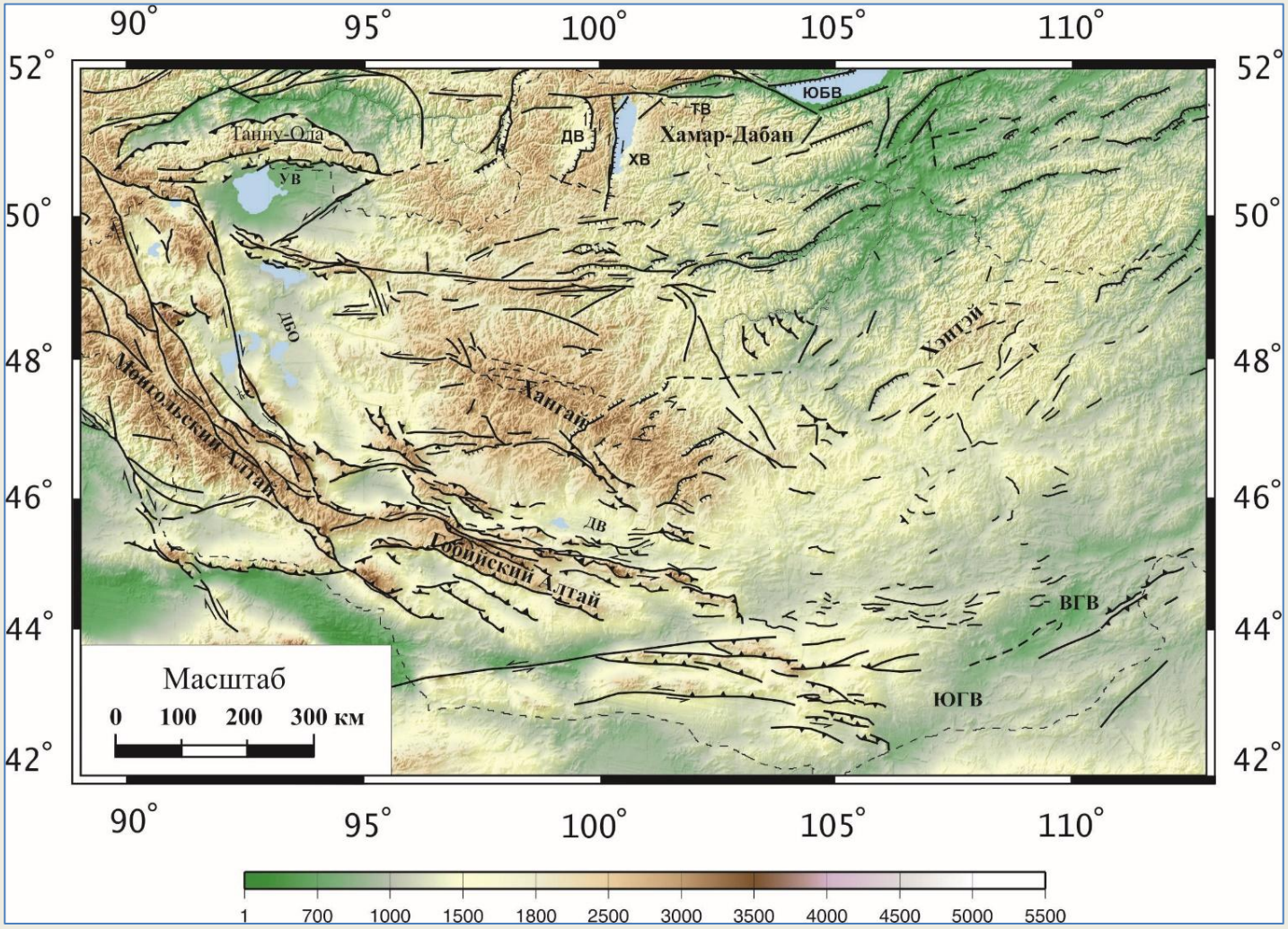

Tectonic-stratigraphy map of the terranes of Mongolia (Badarch et al., 2002)

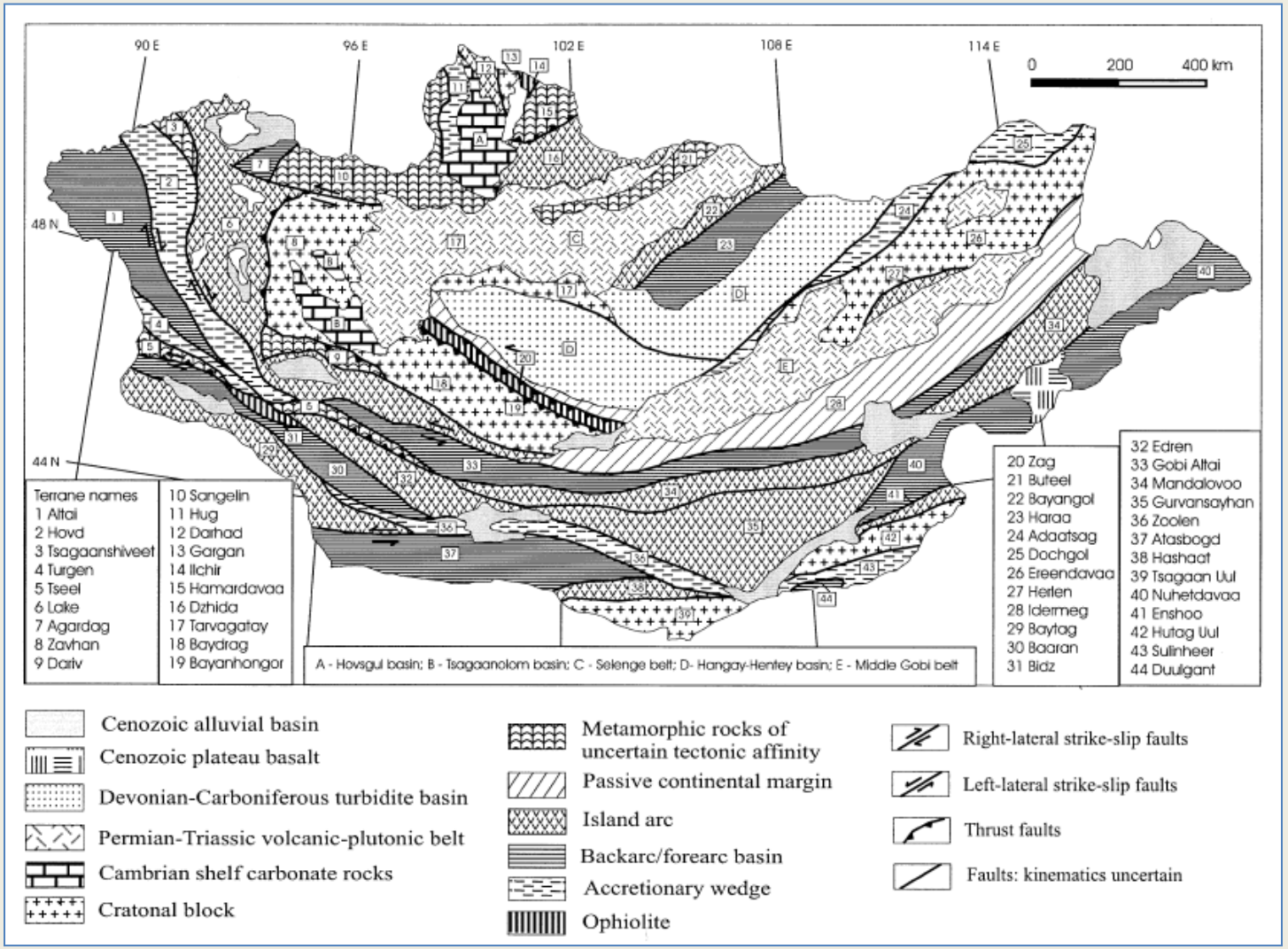

РОССИЙСКАЯ АКАДЕМИЯ НАУК
СИБИРСКОЕ ОТДЕЛЕНИЕ
ИНСТИТУТ ЗЕМНОЙ КОРЫ
Автор: К.Г. Леви
ИРКУТСК 2007

КАРТА НЕОТЕКТОНИКИ СЕВЕРО-ВОСТОЧНОГО СЕКТОРА АЗИИ

MAP OF NEOTECTONIC OF NORTHERN-EAST SECTOR OF ASIA

RUSSIAN ACADEMY OF SCIENCES
SIBERIAN BRANCH
INSTITUTE OF THE EARTH CRUST
Compiled by K.G. Levi
IRKUTSK 2007

КАРТА НЕОТЕКТОНИЧЕСКИХ ДВИЖЕНИЙ
MAP OF NEOTECTONIC MOTIONS

Шкала амплитуд вертикальных движений, м
Scale of amplitudes of neotectonic motions, m

3000
2500
2000
1500
1000
500
0
-1000
-2000
-3000
-4000
-5000
-6000
-7000
-8000

Географические контуры схематизированы
Geographical contours are schematic

Масштаб 1 : 7500000
150 0 150 300 450 600км

Scale 1 : 7500000
150 0 150 300 450 600км

Сдвиги со сбросовой компонентой
Strike-sleep faults with normal component
Сдвиги
Strike-sleep faults
Сдвиги со взбросовой компонентой
Strike-sleep faults with revers component

Границы больших литосферных блоков
Boundaries of big Lithispheric blocks

Кайнозойские вулканические покровы (A) и аппараты центрального типа (B)
Cenozoic volcanic plateau (A) and cinder cones (B).

Кайнозойские седиментационные бассейны. *Cenozoic sedimentary basins.*

Дивергентные *Divergent*
Конвергентные *Convergent*
Трансформные *Transform*

Области повышенной проницаемости литосферы. *Regions with permiability of Lithosphere*

При составлении карты использованы опубликованные материалы: Николаев, 1960; Николаев, Наймарк, 1970; Флоренсов, Варламов, 1981; Погребицкий, 1985; Косыгин, 1985; Хренов, Золотарев, 1979; Логачев, 1984; Леви и др., 1984; и др.

Благодарности: автор благодарит чл.-корр РАН Е.В. Склярова, д.г.-м.н., профессора С.И. Шермана и к.г.-м.н., с.н.с. А.И. Мирошниченко за полезные и доброжелательные советы по оформлению карты
Карта составлена при финансовой поддержке грантов РФФИ 05-05-97251 и НОЦ "Байкал"

СХЕМА РАЙОНИРОВАНИЯ ПО ВРЕМЕНИ НАЧАЛА ПРОЯВЛЕНИЯ НЕОТЕКТОНИЧЕСКИХ ДВИЖЕНИЙ С ЭЛЕМЕНТАМИ СЕЙСМИЧНОСТИ
SCHEME OF ZONING ACCORDING TO BEGINNING NEOTECTONIC MOTIONS

ВРЕМЯ НАЧАЛА ПРОЯВЛЕНИЯ НЕОТЕКТОНИЧЕСКИХ ДВИЖЕНИЙ:
AGE OF ACCORDIN TO BEGINNING OF NEOTECTONIC MOTIONS:

На континентальной литосфере *On Continental Lithosphere*

$K_2 - P_1$	P_1	P_{1-2}	P_{2-3}	P_3	$P_3 - N_1$	$N_1 - N_2$	$N_2 - N_3$	$N_3 - Q_1$

На океанской литосфере *On Ocean Lithosphere*

$P_3 - N_1$	?	$N_2 - N_3$	$N_3 - Q$

Границы областей с различным временем проявления неотектонических движений. *Boundaries of regions with different age of neotectonic motions.*

Сосредоточенная сейсмичность дивергентных границ. *Concentrate seismicity of divergent boundaries.*

Сосредоточенная сейсмичность трансформных границ. *Concentrate seismicity of transform boundaries.*

Сосредоточенная сейсмичность конвергентных границ *Concentrate seismicity of convergent boundaries*

Рассеянная внутриплитная сейсмичность *Disperse intraplate seismicity*

СХЕМАТИЧЕСКАЯ КАРТА ТОЛЩИНЫ ЛИТОСФЕРЫ КОНТИНЕНТОВ И ОКЕАНОВ
SCHEMATIC MAP OF THICKNESS OF LITHOSPHERE OF CONTINENTS AND OCEANS

Толщина континентальной литосферы, вычисленная как *L(q)*
Thickness of Continental Lithosphere
25-50 км | 50-75 км | 75-100 км | 100-125 км | 125-150 км | 150-175 км | 175-200 км

Толщина океанской литосферы, вычисленная как *L(t)*
Thickness of Lithosphere of Oceans
< 10 км | 10-30 км | 30-60 км | 60-90 км | > 90 км

- The main goal: To identify the main patterns of stress-strain state of the earth's crust of the Mongolian Altai and its evolution in the Cenozoic
- The main tasks:
- 1. Reconstruct the paleostress state based on data on tectonic fracturing in active fault zones and folding in MZ and KZ sediments; supplement the database "Maps of the stress state of the earth's crust in Mongolia"
- 2. Compare the paleostress state with data on the modern field of tectonic stresses and deformations based on data on earthquake focal mechanisms and satellite geodesy
- 3. Conduct modeling of the modern stress-strain state and kinematics of active faults using the finite element method

Scheme of the study of the Cenozoic stress state of the earth's crust in the territory of Mongolia and southern Siberia using geological and structural methods

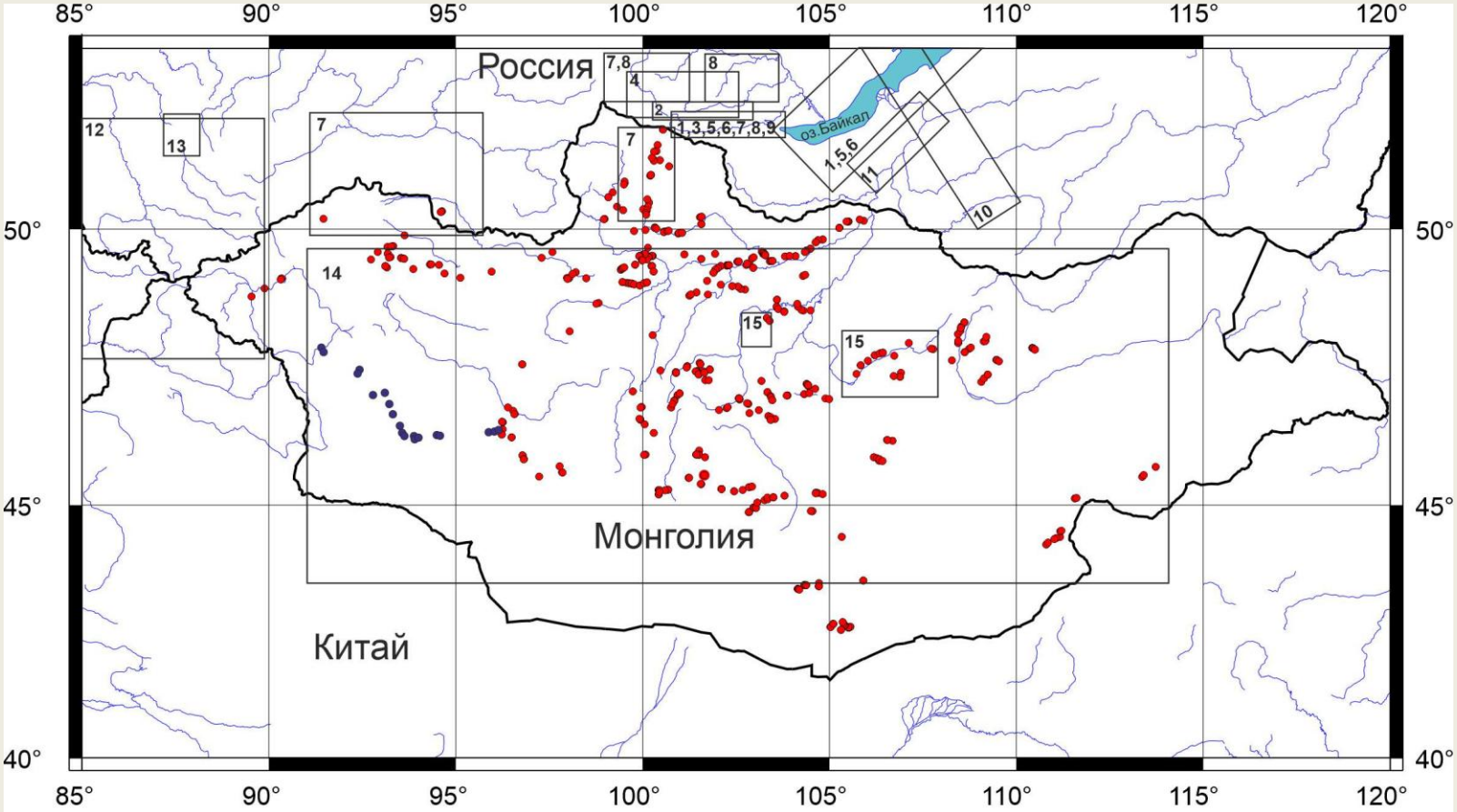

1 Шерман и др. 1973, Шерман, Днепровский 1986, 1989
2 Ружич и др. 1972, Ружич 1978, Ружич, Хилько 1985
3 Рязанов 1978
4 Рассказов 1989, 1993
5 Delvaux et al., 1997
6 Sankov et all., 1996, 1997
7 Парфеевец, Саньков, 2006, Парфеевец и др. 2002, Саньков, Парфеевец, 2005
8 Аржанникова и др., 2011, 2007, Arzhannikova et al., 2004, Аржанникова, Аржанников, 2005
9 Лунина, Гладков, 2004; Лунина и др., 2009
10 Семинский и др., 2012, Семинский и др., 2013, Черемных, 2010, Черемных, 2012
11 Лунина, Гладков, 2009, Лунина и др., 2009
12 Дельво и др., 1995; Delvaux et al., 2013
13 Dehandschutter et al., 2002
14 Levi et al., 2004
15 Семинский и др., 2017

Точки наблюдений наших исследований на территории Монголии за период 1998 – 2019 г.г.

Точки наблюдений наших исследований на территории Монголии в 2023 г.

Method of reconstruction of paleo- and modern stress state

- Data: (1) planes of ruptures and directions of displacement along them in zones of active faults, MZ and KZ rocks and sediments; (2) rupture planes in earthquake foci
- Calculation using the program TENSOR (Delvaux, 1993) – “right dihedra” method + rotation optimization => σ1, σ2, σ3 and staress-ratio

$$R=(\sigma 2-\sigma 3)/(\sigma 1-\sigma 3)$$

Classification of stress tensors (Delvaux et al., 1997)

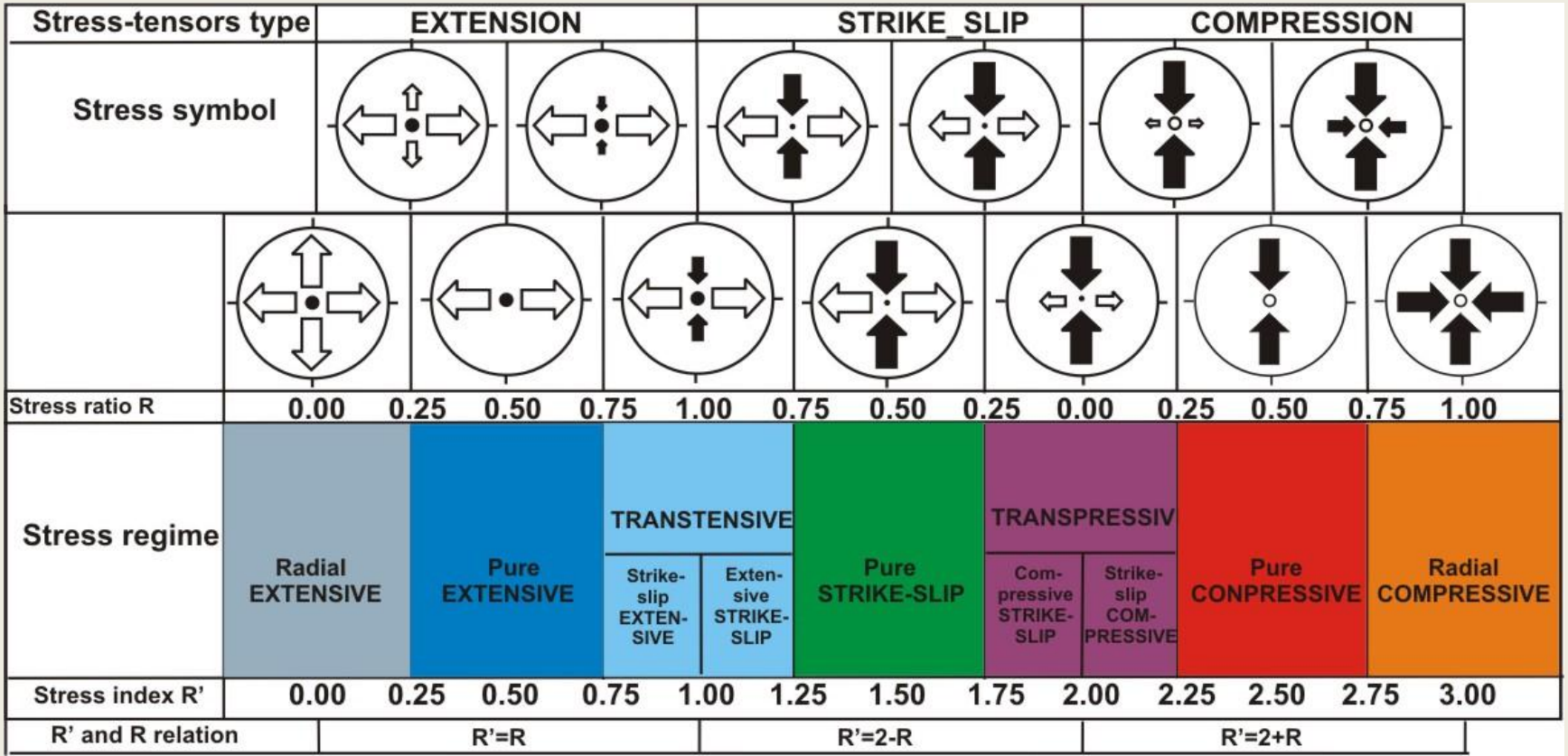

Stress tensors of Kobdo, Sagsay and Tsagan-Shibety fault zones

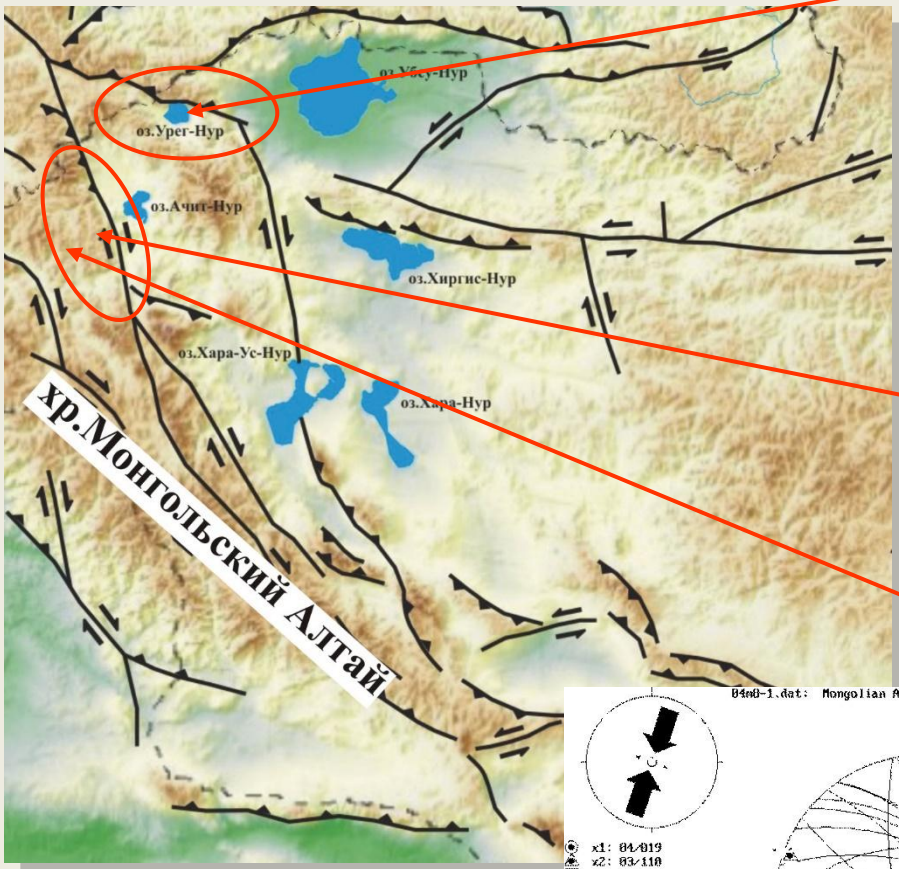

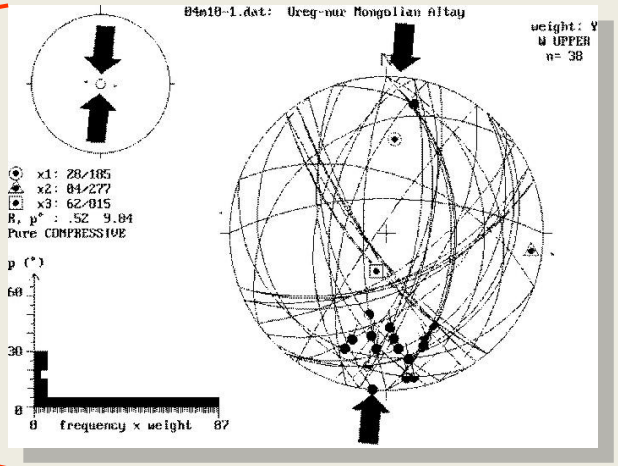

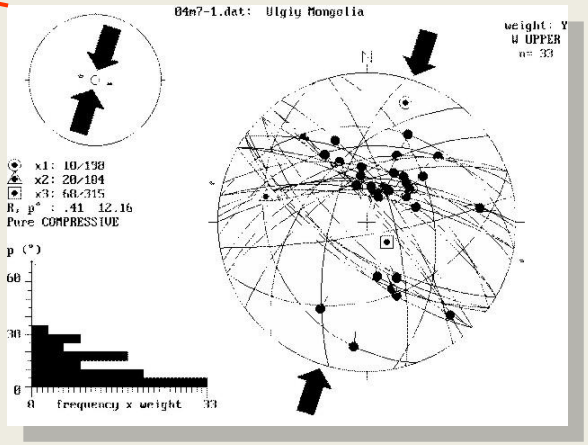

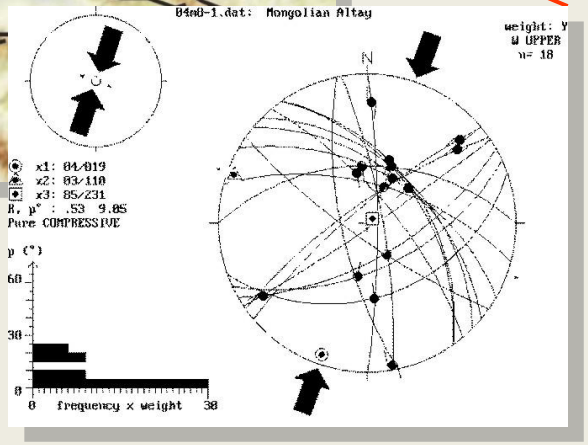

Late Cenozoic right lateral movements along Kobdo fault

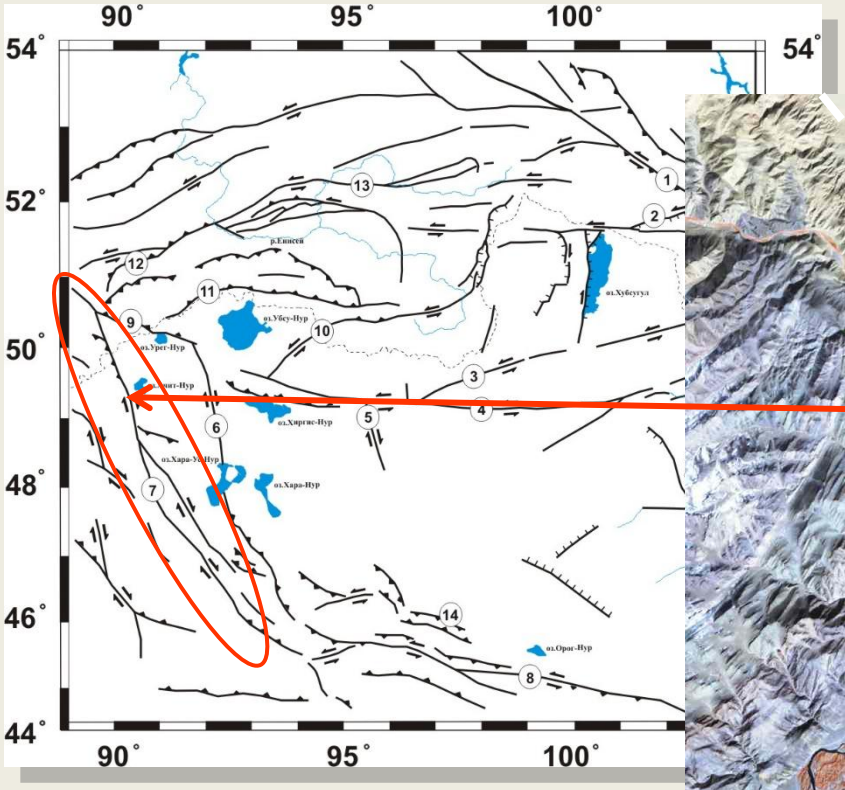

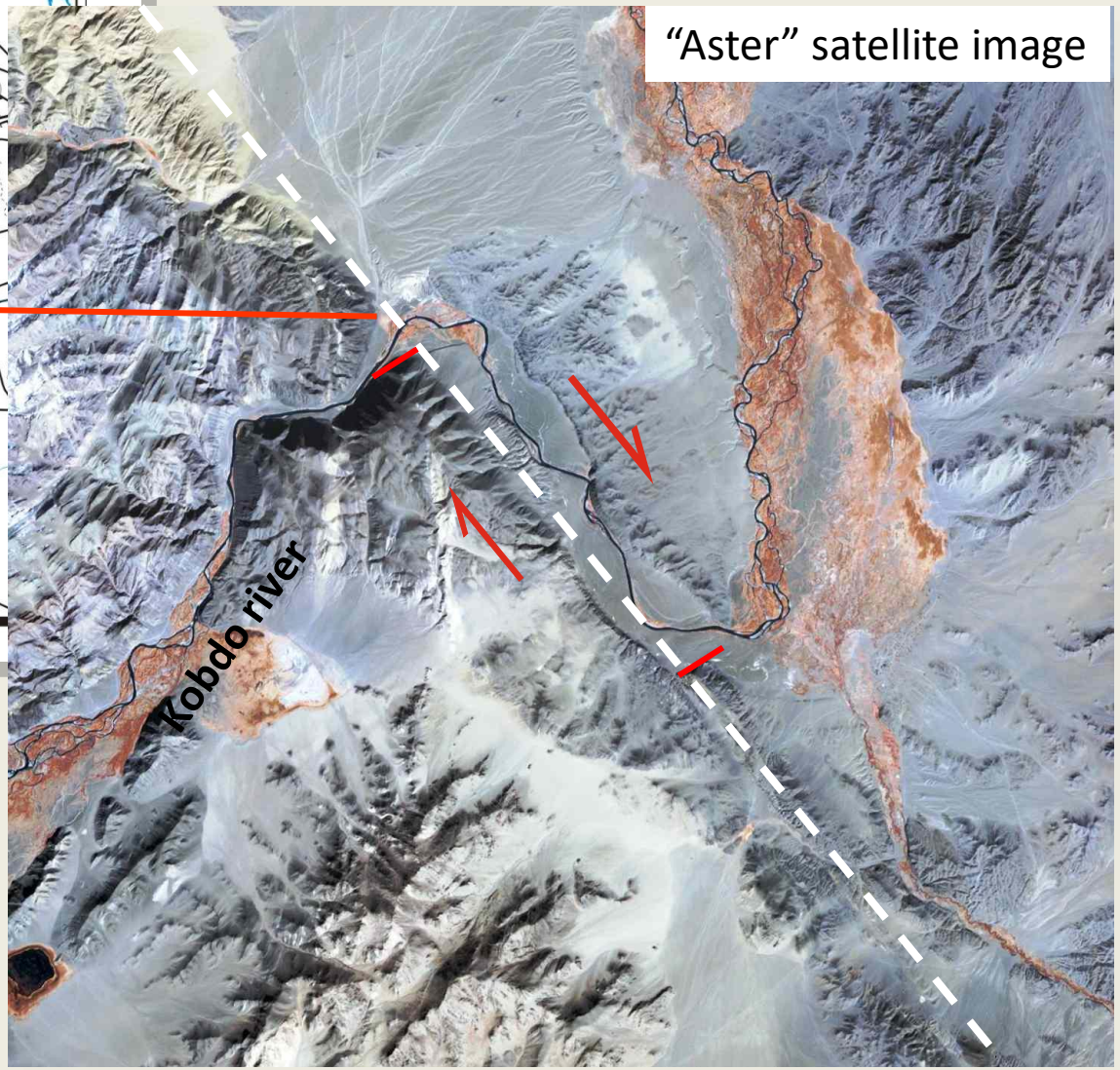

Amplitude of horizontal
Movement - 8600 m

Tectonic fracturing in Pliocene lacustrine clays in the Kobdo fault zone

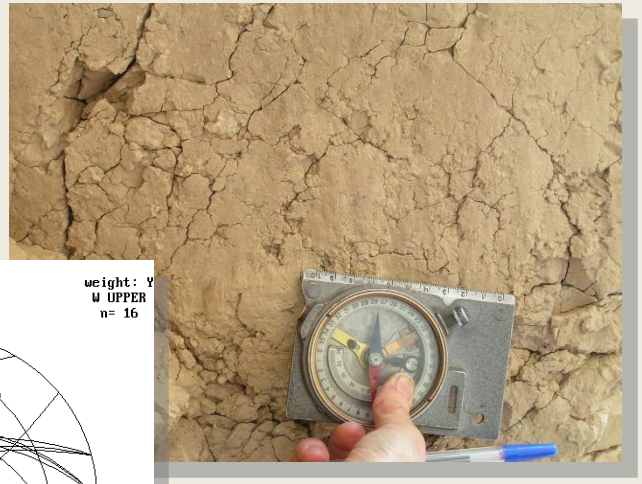

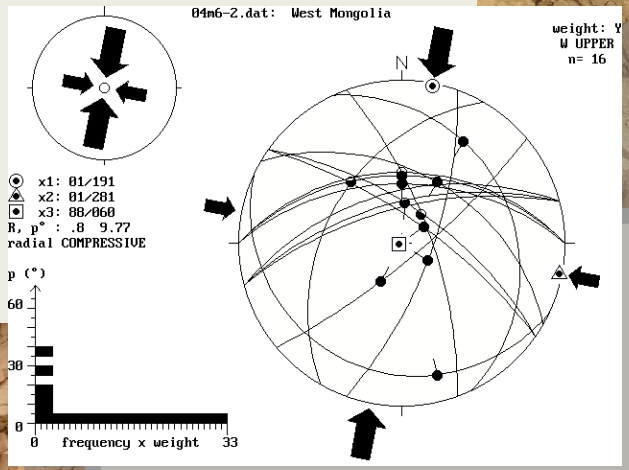

1

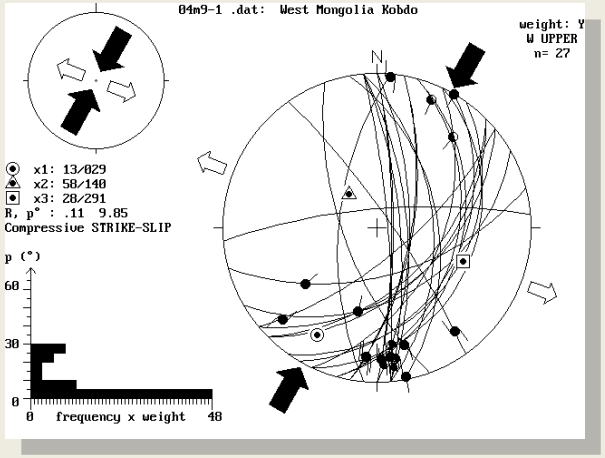

2

Stress tensors of Khan-Tayshir-Nuruu fault system

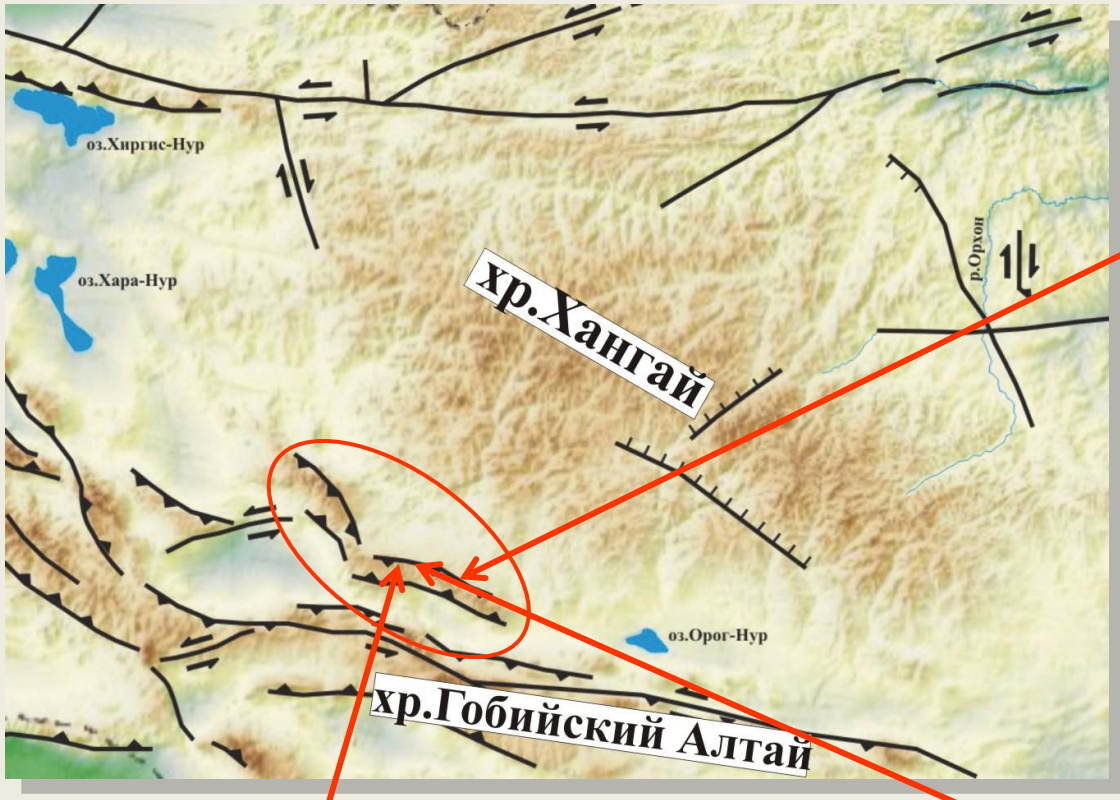

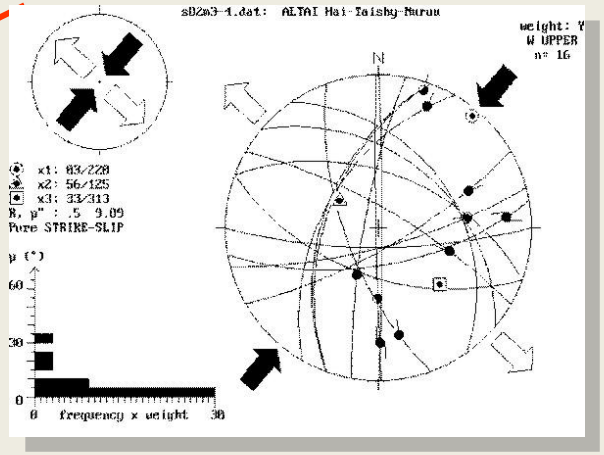

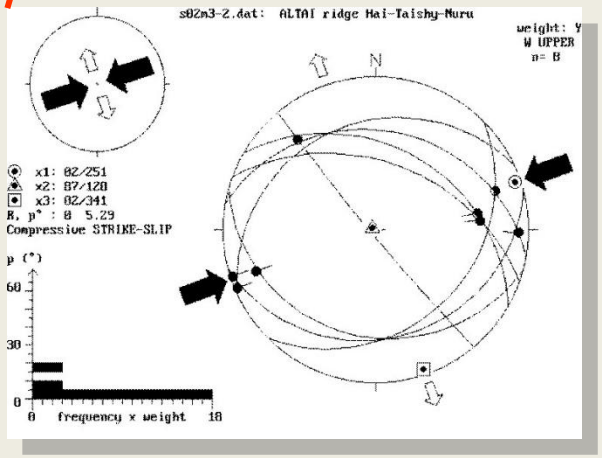

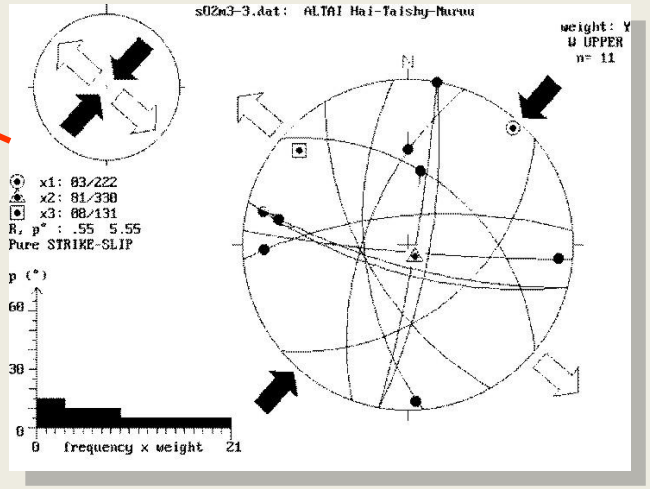

Location of research sites

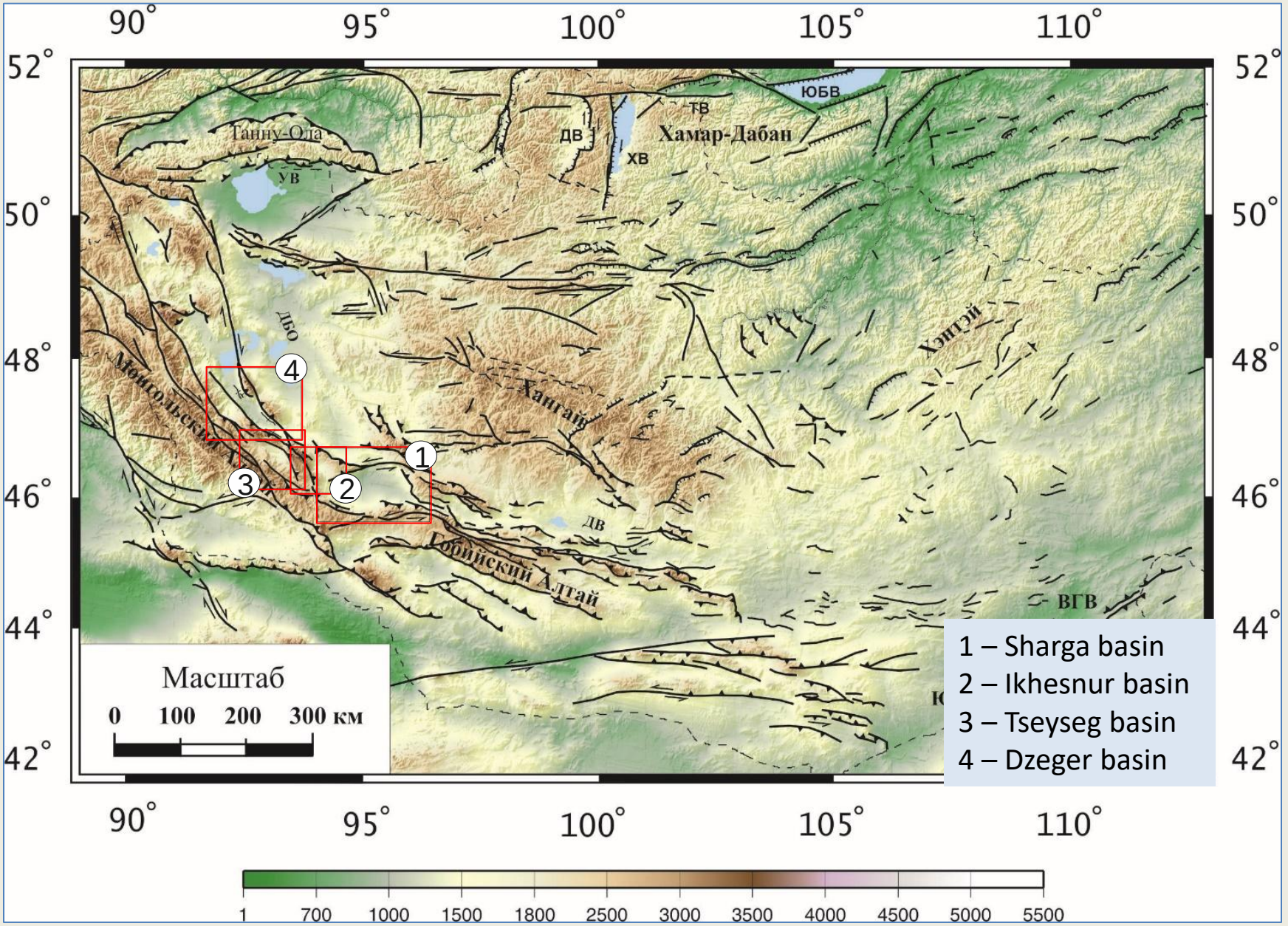

Characteristics of sediments of the Mesozoic-Cenozoic basins of the Mongolian Altai (by Nikolaeva, Shuvalov, 1969)

MZ			KZ		
J_{1-2}	J_3	K_1	Pg олигоцен	N миоцен-плиоцен	Q плейстоцен-голоцен
Large-pebble, boulder conglomerates with interlayers and lenses of coarse-grained sandstones and gravelites, gray-colored inequigranular sandstones interbedded with small-pebble conglomerates, greenish-gray siltstones, fine-grained sandstones with interlayers of carbonaceous siltstones, gray and pink lacustrine limestones, red-colored siltstones and sandstones. In the marginal parts of the basins there are coarse-grained deposits of proluvial facies: boulder conglomerates, fanglomerates, conglobreccias with interlayers and lenses of inequigranular sandstones, gravelites and packs of coarse-grained sandstones.	Coarse-grained red-colored conglobreccias and conglomerates weakly cemented by coarse-grained sandy material with interlayers and lenses of gravelstones and coarse-grained sandstones with cross-bedding.	Grey-colored sandstones, siltstones with calcareous cement and with thin interlayers of fine-pebble conglomerates and coarse-grained sandstones.	Loose red sands and loams with thin basal pebbles at the base.	Coarse-grained light grey sands and pebbles.	Pebble-boulder, pebble, sand-gravel alluvial-proluvial deposits of alluvial fans and foothills (belays).


N_2-Q

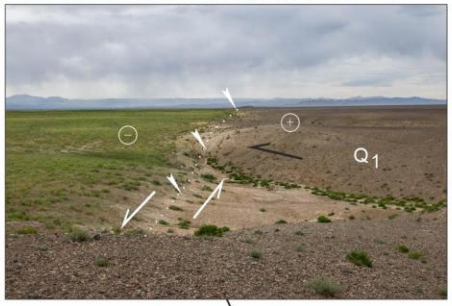
Q_1

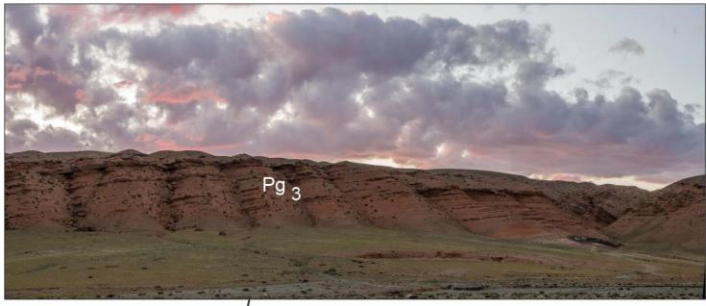
Pg_3

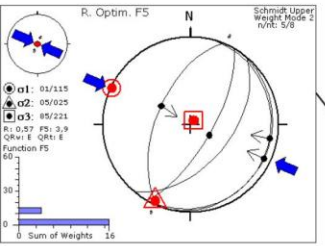
R. Optim. FS
N
Schmidt Upper
Weight Mode 2
n/nt: 5/6
σ1: 01/115
σ2: 05/025
σ3: 85/221
R: 0,57 FS: 3,9
QRw: E QRt: E
Function FS
60
30
0
0 Sum of Weights 16

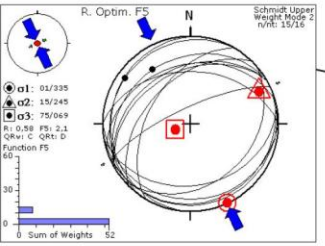
R. Optim. FS
N
Schmidt Upper
Weight Mode 2
n/nt: 15/16
σ1: 01/335
σ2: 15/245
σ3: 75/069
R: 0,58 FS: 2,1
QRw: C QRt: D
Function FS
60
30
0
0 Sum of Weights 52

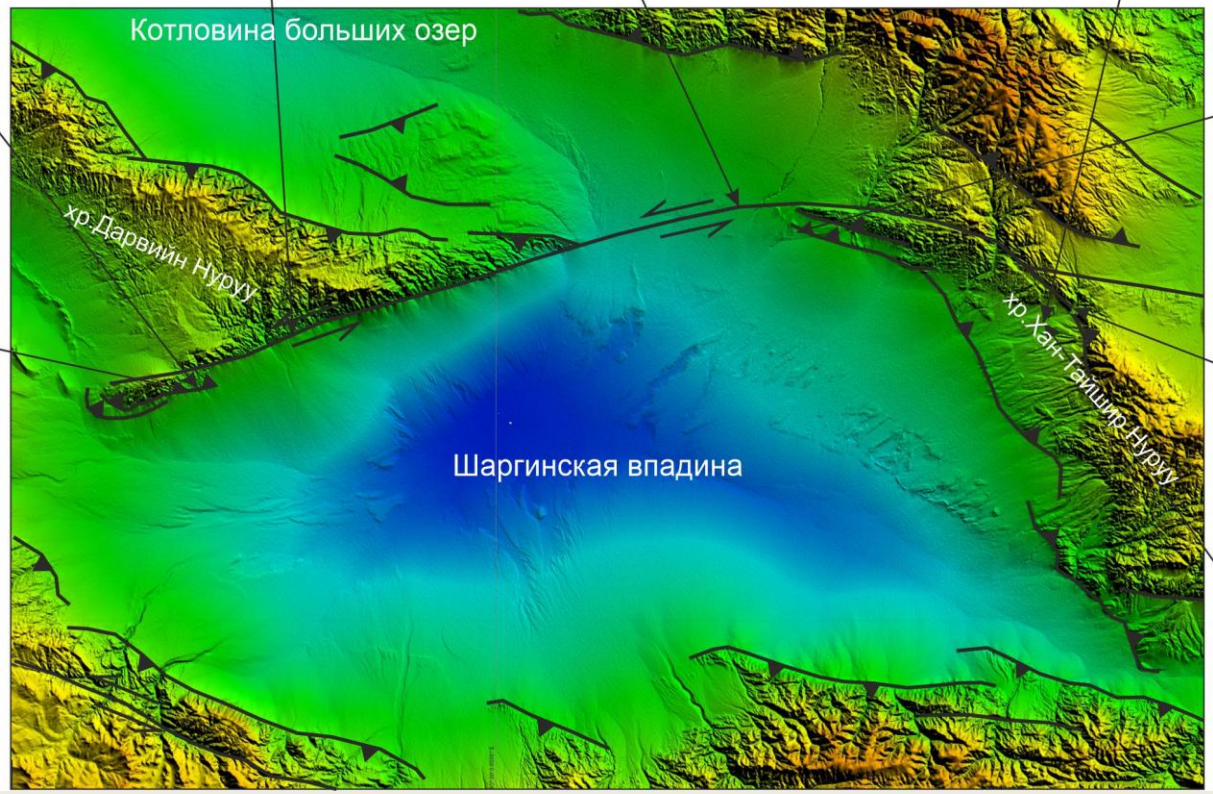
Котловина больших озер
хр.Дарвийн Нуруу
Шаргинская впадина
хр.Хан-Тайшир-Нуруу

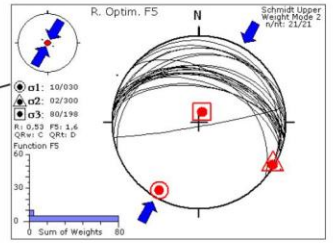
R. Optim. FS
N
Schmidt Upper
Weight Mode 2
n/nt: 21/21
σ1: 10/030
σ2: 02/300
σ3: 80/198
R: 0,53 FS: 1,6
QRw: C QRt: D
Function FS
60
30
0
0 Sum of Weights 80

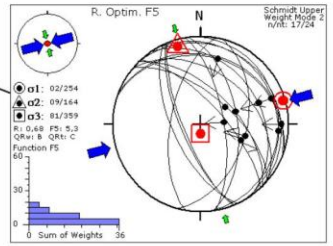
R. Optim. FS
N
Schmidt Upper
Weight Mode 2
n/nt: 17/24
σ1: 02/254
σ2: 09/164
σ3: 81/359
R: 0,68 FS: 5,3
QRw: B QRt: C
Function FS
60
30
0
0 Sum of Weights 36

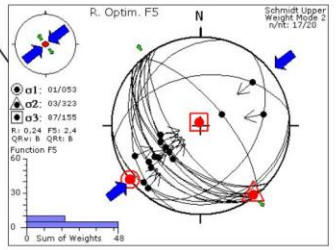
R. Optim. FS
N
Schmidt Upper
Weight Mode 2
n/nt: 17/20
σ1: 01/053
σ2: 03/323
σ3: 87/155
R: 0,24 FS: 2,4
QRw: B QRt: B
Function FS
60
30
0
0 Sum of Weights 48

Folded and faulted deformations in the northern side of the Sharga depression

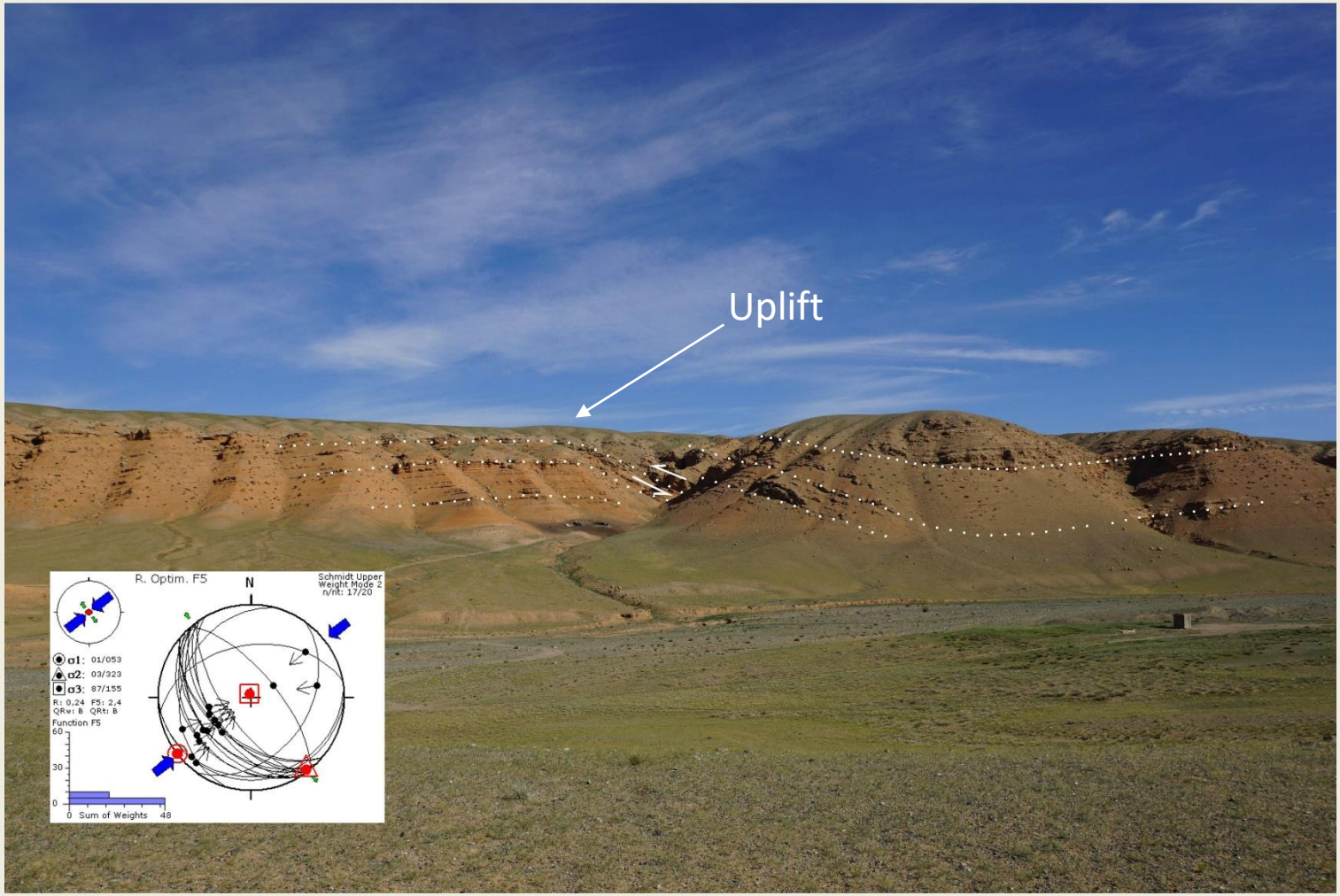


J_3- K_1

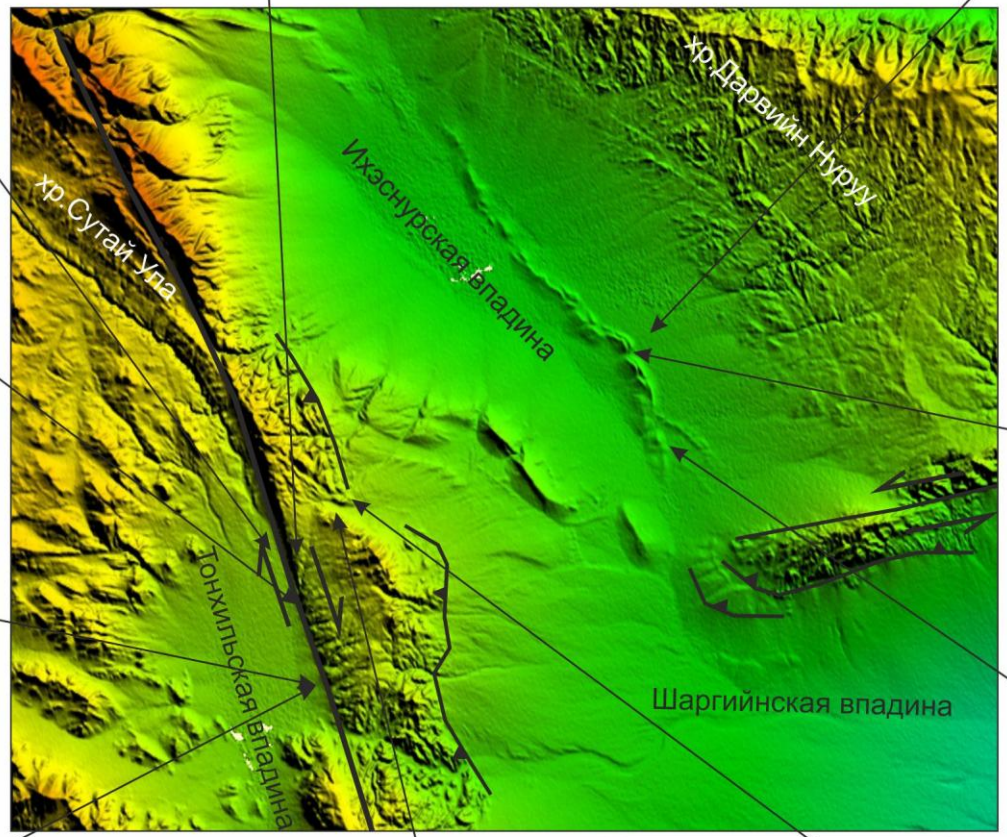
хр.Сутай Ула
Ихаснурская впадина
хр.Дарвийн Нуруу
Тонхильская впадина
Шаргийнская впадина

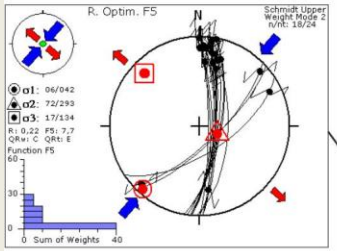
R. Optim. FS
Schmidt Upper Weight Mode 2
n/nt: 18/24
α1: 06/042
α2: 72/293
α3: 17/134
Function FS
Sum of Weights

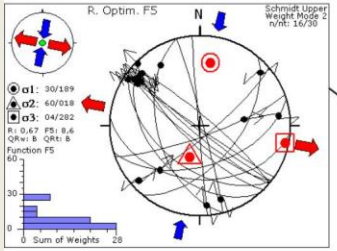
R. Optim. FS
Schmidt Upper Weight Mode 2
n/nt: 16/30
α1: 30/189
α2: 60/018
α3: 04/282
Function FS
Sum of Weights

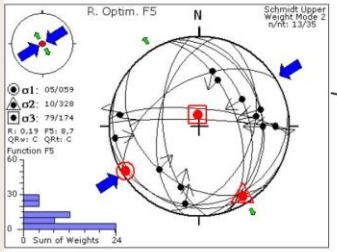
R. Optim. FS
Schmidt Upper Weight Mode 2
n/nt: 13/35
α1: 05/059
α2: 10/328
α3: 79/174
Function FS
Sum of Weights

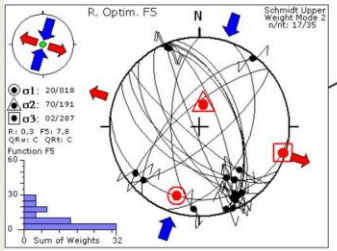
R. Optim. FS
Schmidt Upper Weight Mode 2
n/nt: 17/35
α1: 20/018
α2: 70/191
α3: 02/287
Function FS
Sum of Weights

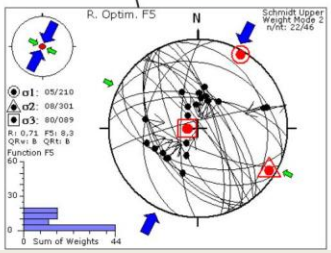
R. Optim. FS
Schmidt Upper Weight Mode 2
n/nt: 22/46
α1: 05/210
α2: 08/301
α3: 80/089
Function FS
Sum of Weights

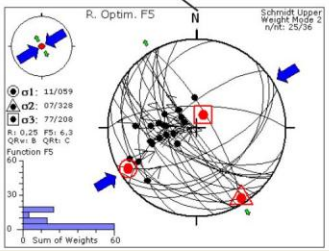
R. Optim. FS
Schmidt Upper Weight Mode 2
n/nt: 25/36
α1: 11/059
α2: 07/328
α3: 77/208
Function FS
Sum of Weights

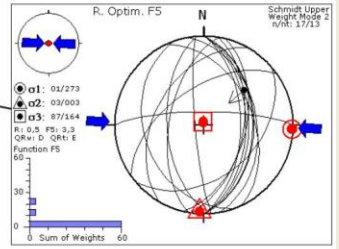
R. Optim. FS
Schmidt Upper Weight Mode 2
n/nt: 17/13
α1: 01/273
α2: 03/003
α3: 87/164
Function FS
Sum of Weights

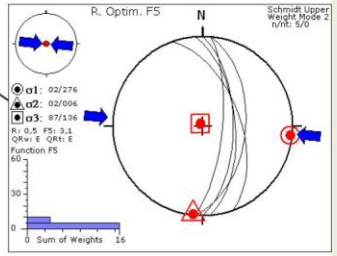
R. Optim. FS
Schmidt Upper Weight Mode 2
n/nt: 5/0
α1: 02/276
α2: 02/006
α3: 87/136
Function FS
Sum of Weights

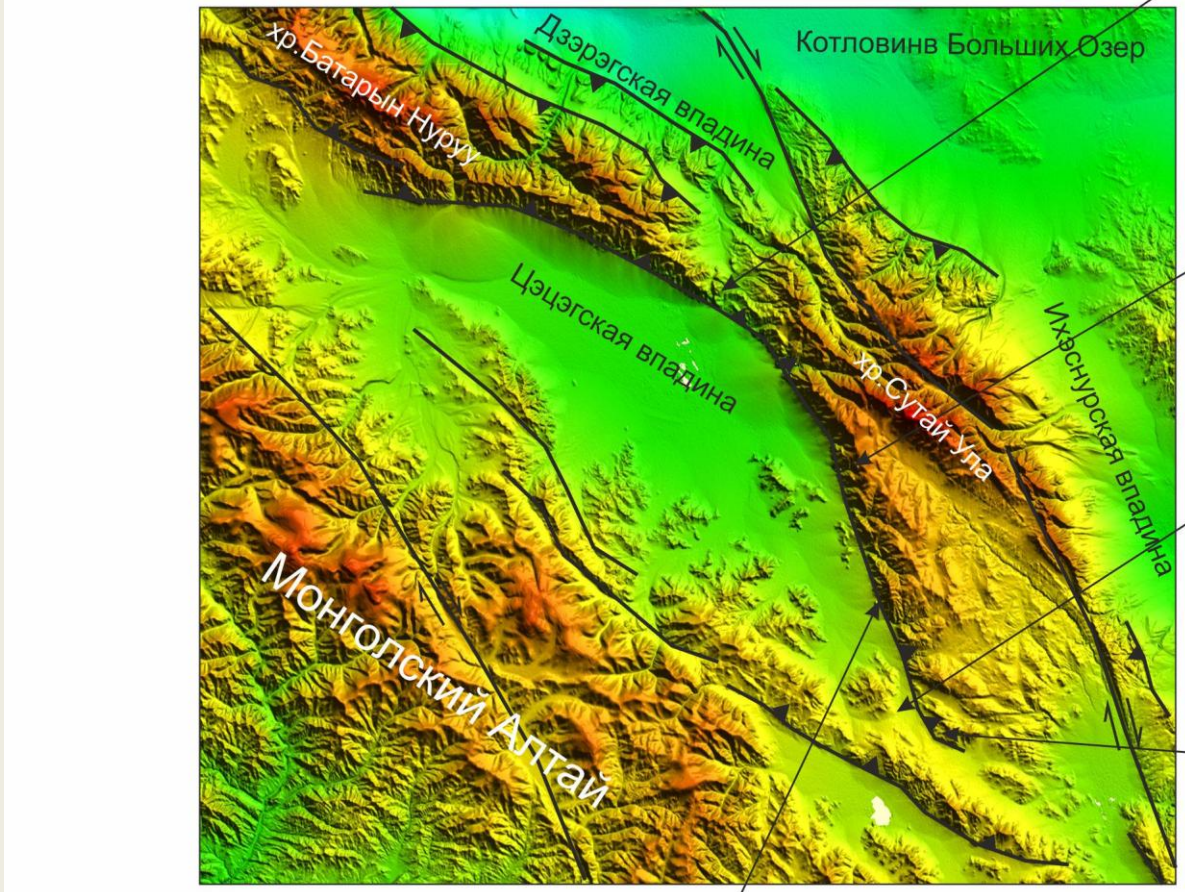
хр.Батарын Нуруу
Дзэрэгская впадина
Котловинв Больших Озер
Цэцэгская впадина
хр.Сутай Уул
Ихэснурская впадина
Монгольский Алтай

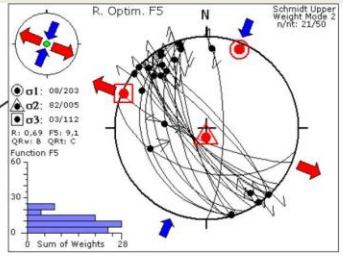
R. Optim. F5
N
Schmidt Upper
Weight Mode 2
n/nt: 21/50
σ1: 08/203
σ2: 82/005
σ3: 03/112
R: 0,69 F5: 9,1
QRw: B QRt: C
Function F5
Sum of Weights 28

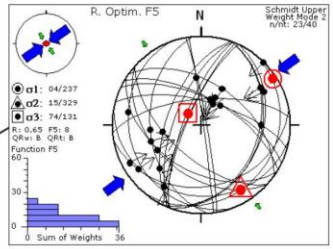
R. Optim. F5
N
Schmidt Upper
Weight Mode 2
n/nt: 23/40
σ1: 04/237
σ2: 15/329
σ3: 74/131
R: 0,65 F5: 8
QRw: B QRt: B
Function F5
Sum of Weights 36

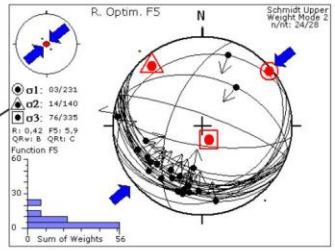
R. Optim. F5
N
Schmidt Upper
Weight Mode 2
n/nt: 24/28
σ1: 03/231
σ2: 14/140
σ3: 76/335
R: 0,42 F5: 5,9
QRw: B QRt: C
Function F5
Sum of Weights 56

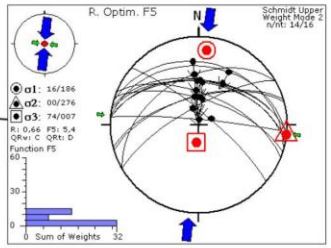
R. Optim. F5
N
Schmidt Upper
Weight Mode 2
n/nt: 14/16
σ1: 16/186
σ2: 00/276
σ3: 74/007
R: 0,66 F5: 5,4
QRw: C QRt: D
Function F5
Sum of Weights 32


J1-2
Pg3- N1-2

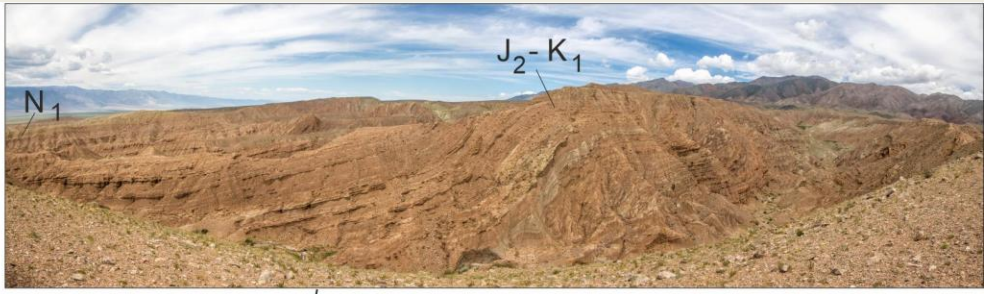
J2- K1
N1

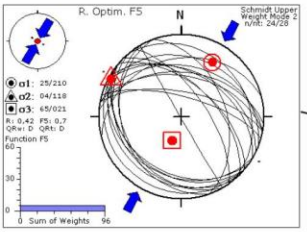
R. Optim. F5
Schmidt Upper Weight Mode 2
n/nt: 24/29
σ1: 25/210
σ2: 04/118
σ3: 65/021
Function F5
Sum of Weights 96

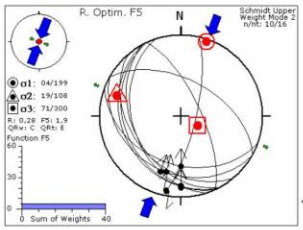
R. Optim. F5
Schmidt Upper Weight Mode 2
n/nt: 10/16
σ1: 04/199
σ2: 19/108
σ3: 71/300
Function F5
Sum of Weights 40

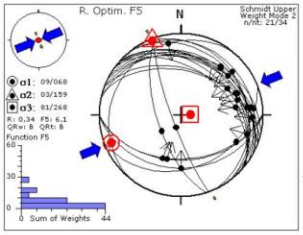
R. Optim. F5
Schmidt Upper Weight Mode 2
n/nt: 21/34
σ1: 09/068
σ2: 03/159
σ3: 81/268
Function F5
Sum of Weights 44

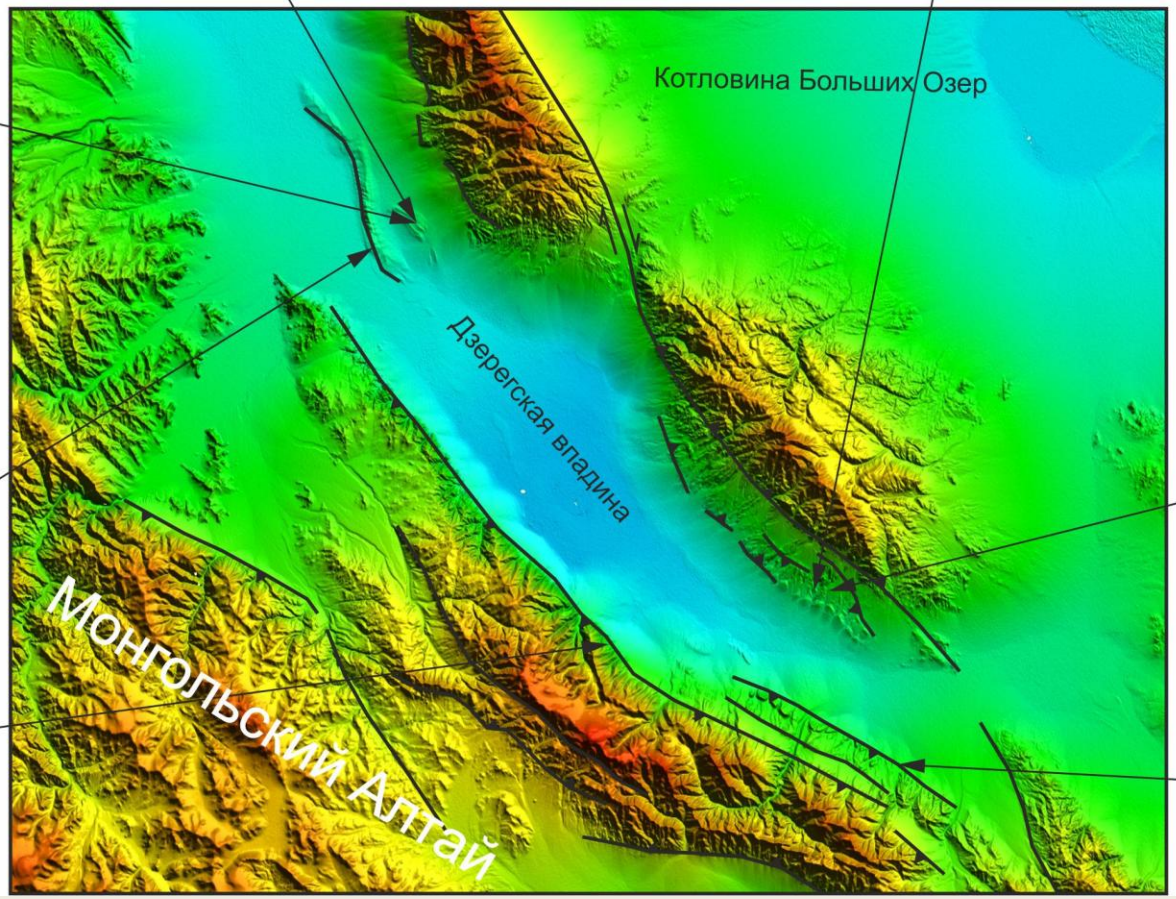
Котловина Больших Озер
Дзерегская впадина
Монгольский Алтай

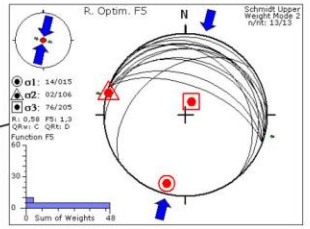
R. Optim. F5
Schmidt Upper Weight Mode 2
n/nt: 13/13
σ1: 14/015
σ2: 02/106
σ3: 76/205
Function F5
Sum of Weights 48

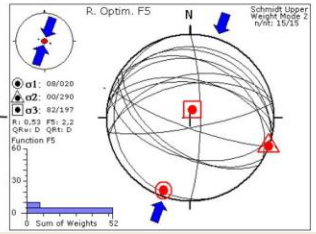
R. Optim. F5
Schmidt Upper Weight Mode 2
n/nt: 15/15
σ1: 08/020
σ2: 00/290
σ3: 82/197
Function F5
Sum of Weights 52

Deformation regimes of the earth's crust within neotectonic structural domains of the territory of the south and west of Mongolia

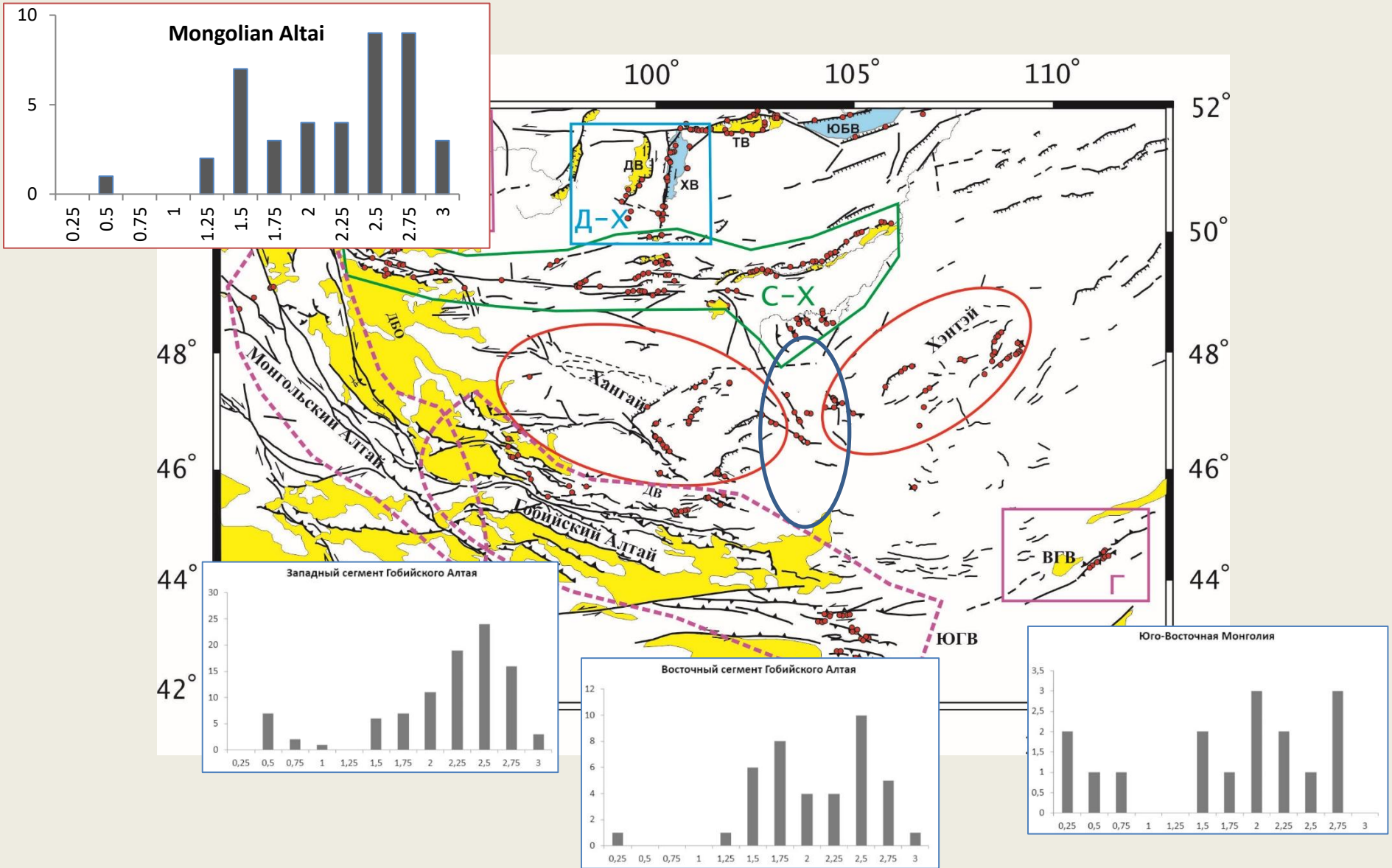

Current stress state of the earth's crust in the Mongolian-Siberian region: earthquake focal mechanisms

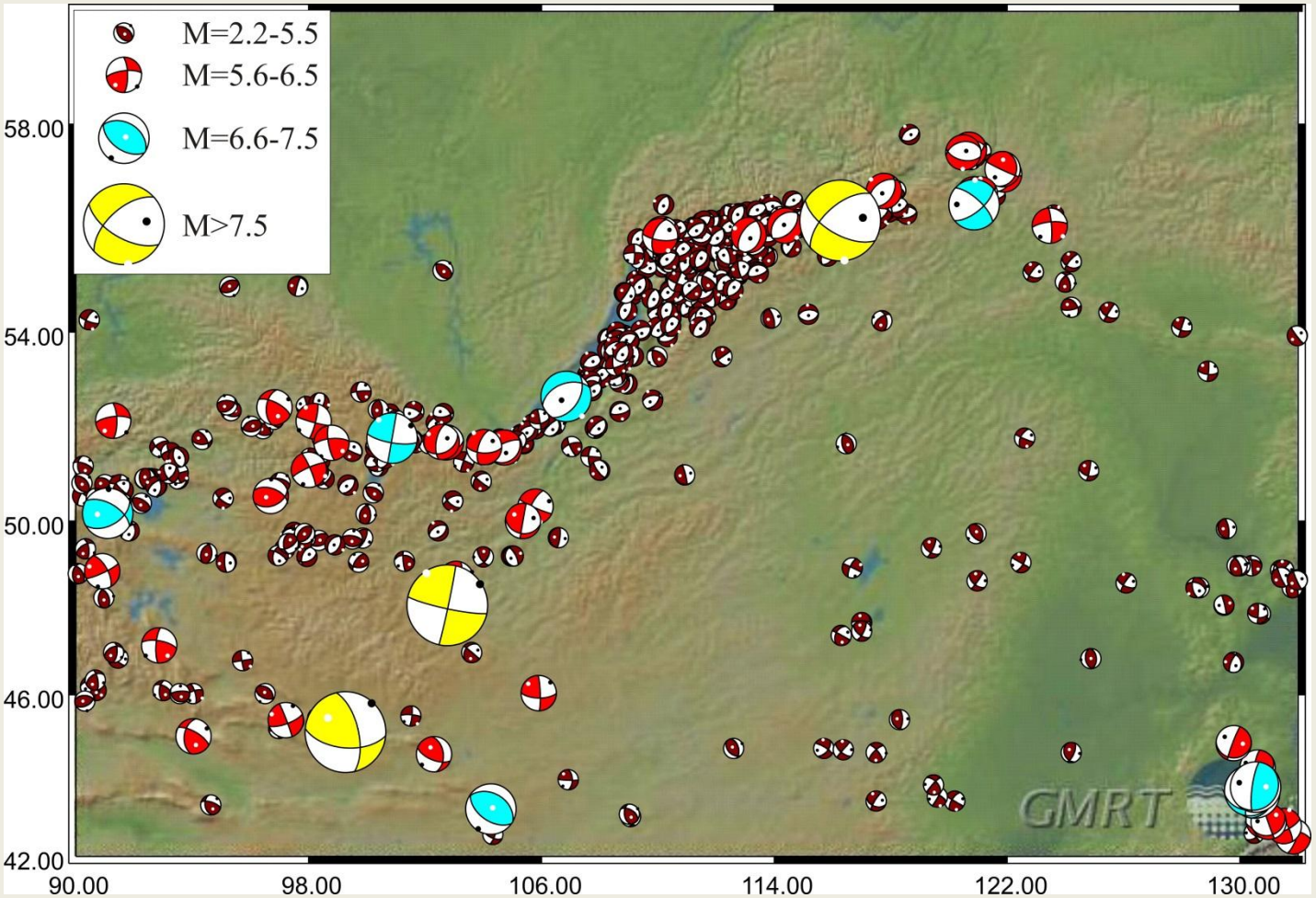

Scheme of the present day stress state of the earth's crust in the Mongolian-Siberian region

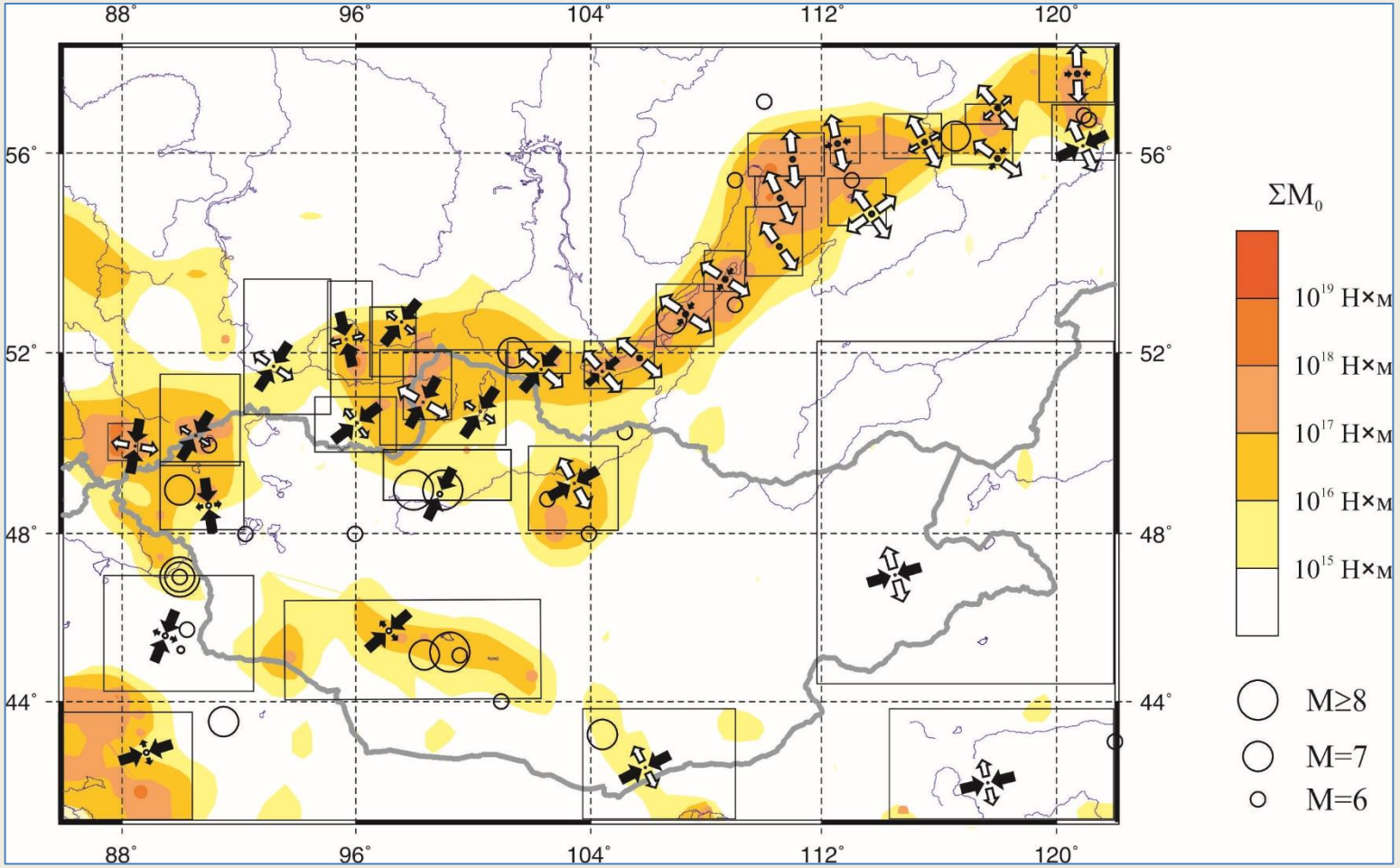

Scheme of zoning of the territory of Mongolia by the type of stress fields of the earth's crust in the late Cenozoic

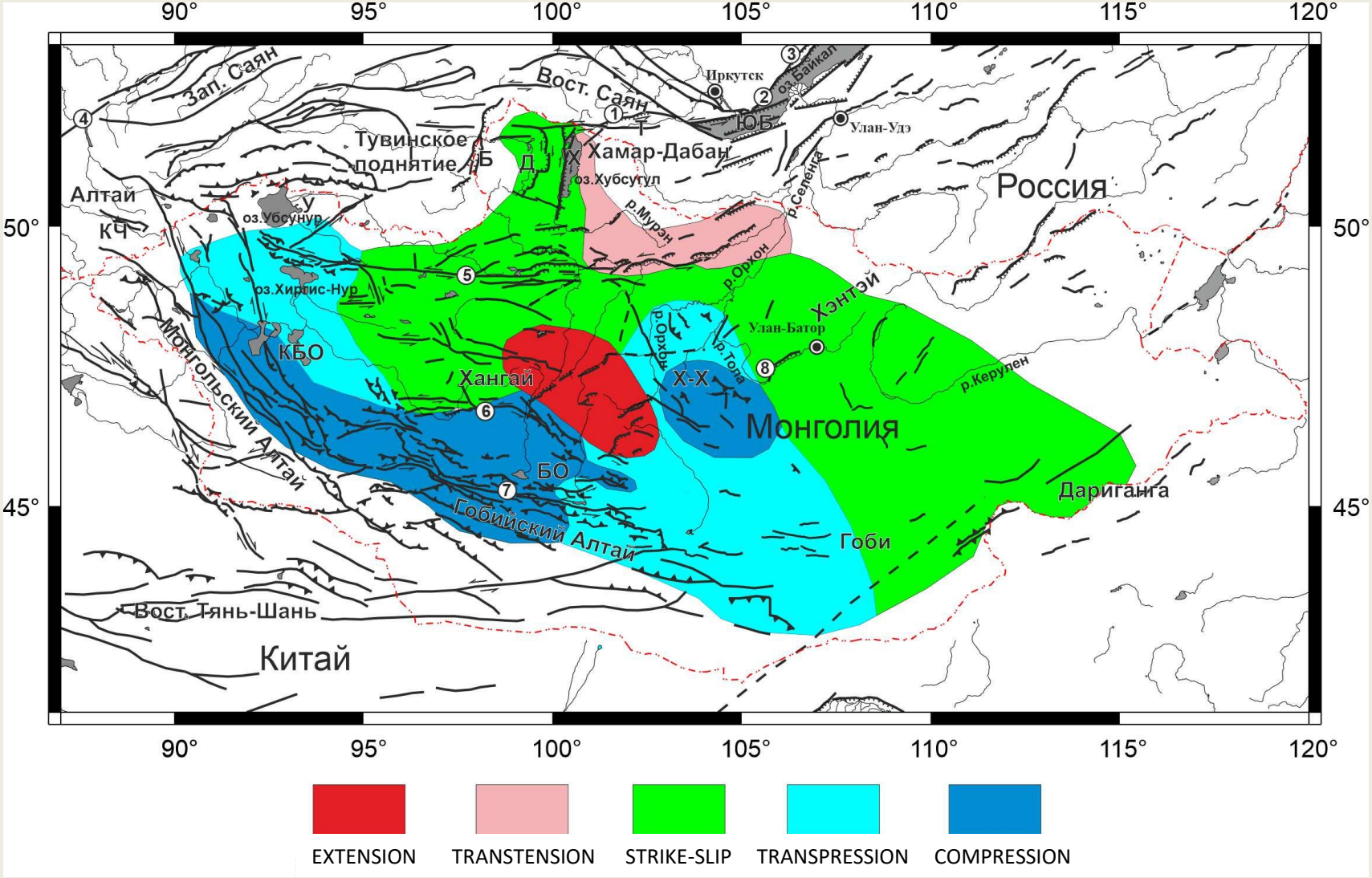

The extension of the axes of maximum horizontal compression SHmax stress tensors reconstructed by geological-structural methods in the territory of Mongolia

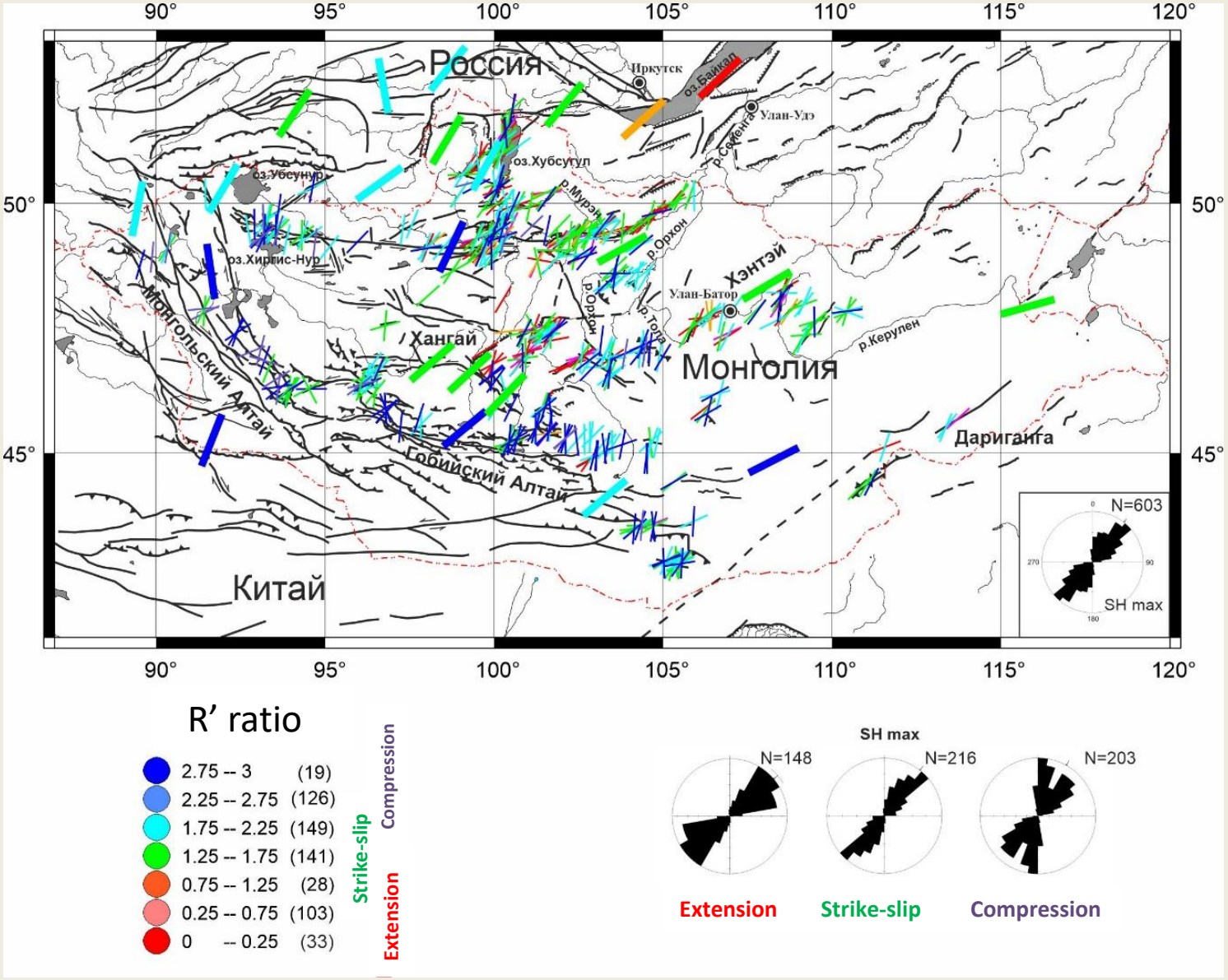

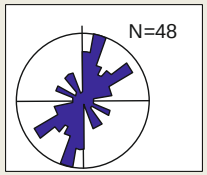

Mongolian Altai

Velocity field of modern horizontal movements of Central Asia for 1994-2004 according to satellite geodesy data (IRKT stable)

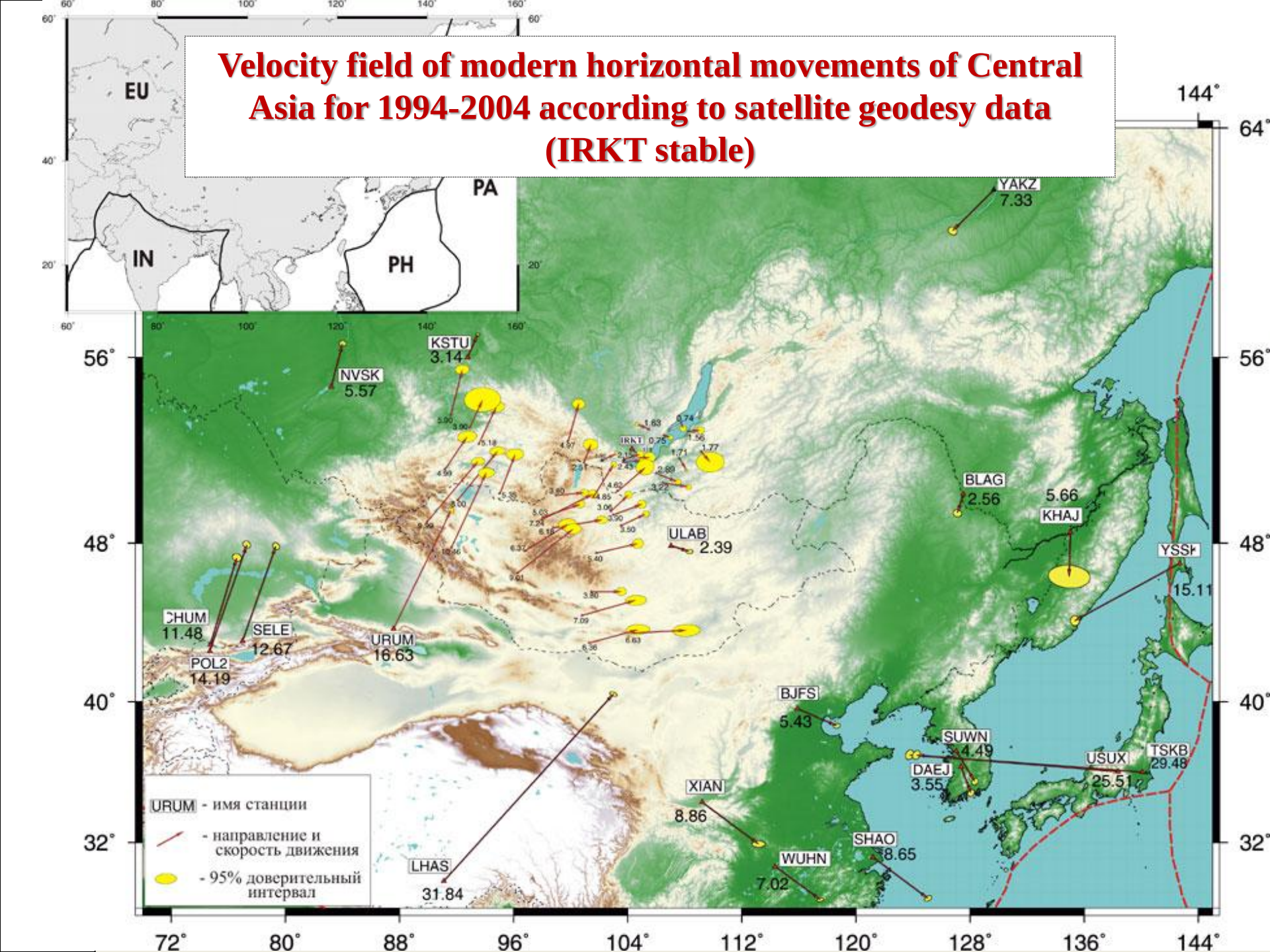

Velocity field of present day horizontal deformations of the earth's surface in the Mongolian-Siberian region based on satellite geodesy data (Lukhnev et al., 2010)

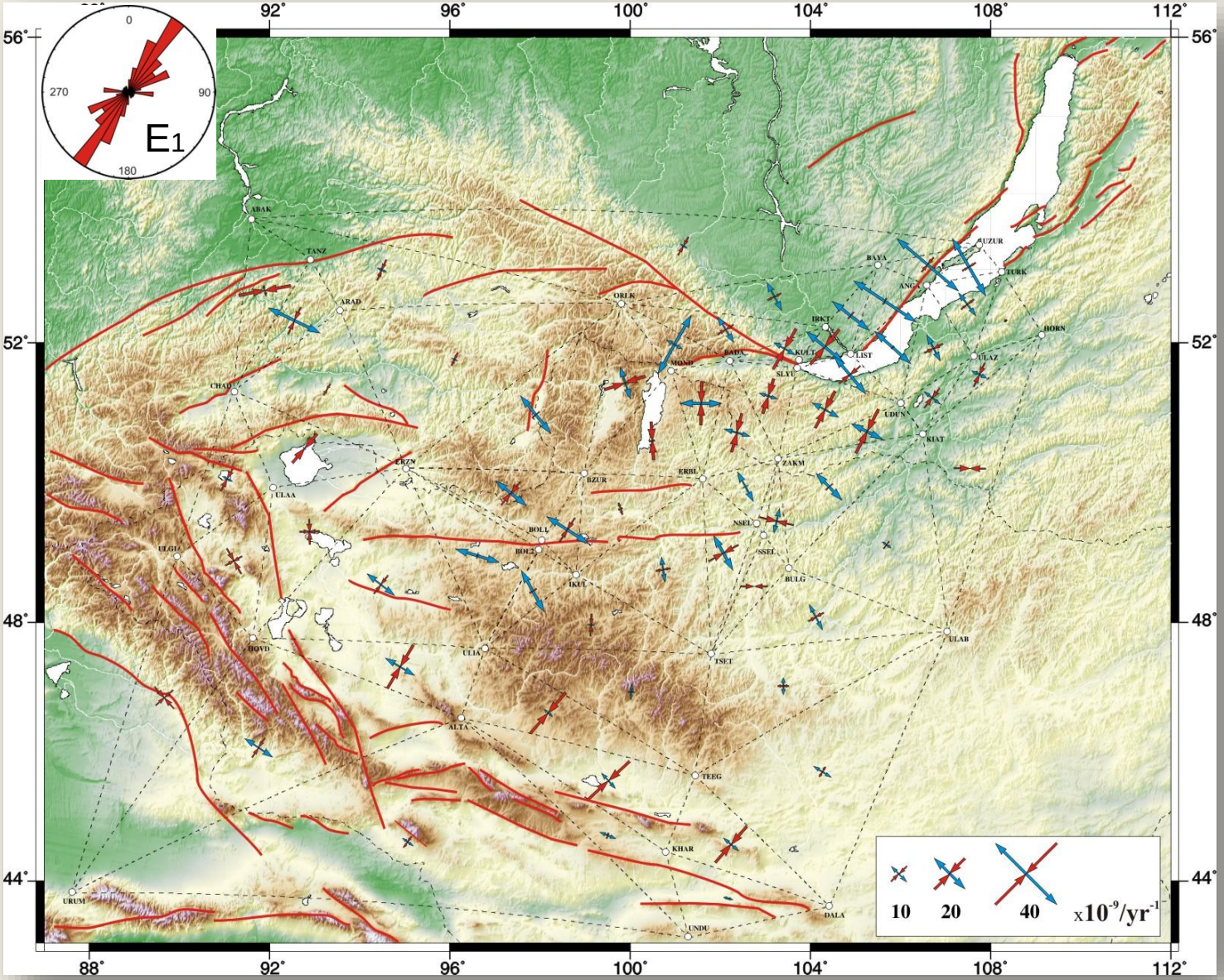

Modeling of stress-strain state of Mongolian Altai and surrounding structures using finite element method

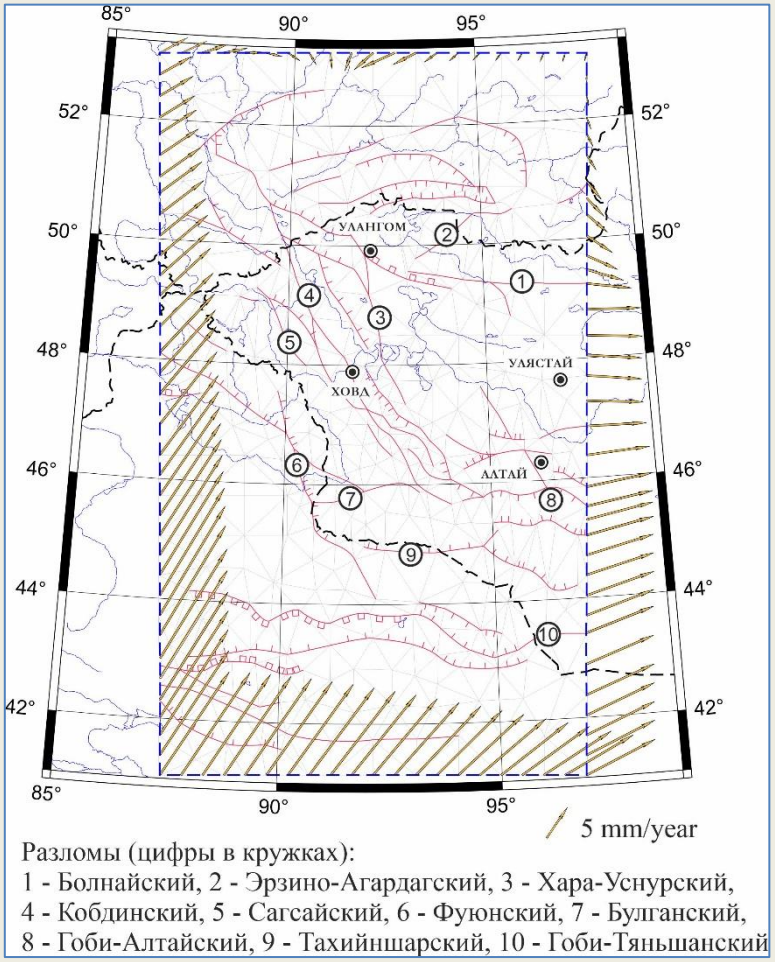

Разломы (цифры в кружках):
1 - Болнайский, 2 - Эрзино-Агардагский, 3 - Хара-Уснурский,
4 - Кобдинский, 5 - Сагсайский, 6 - Фуюнский, 7 - Булганский,
8 - Гоби-Алтайский, 9 - Тахийншарский, 10 - Гоби-Тяньшанский

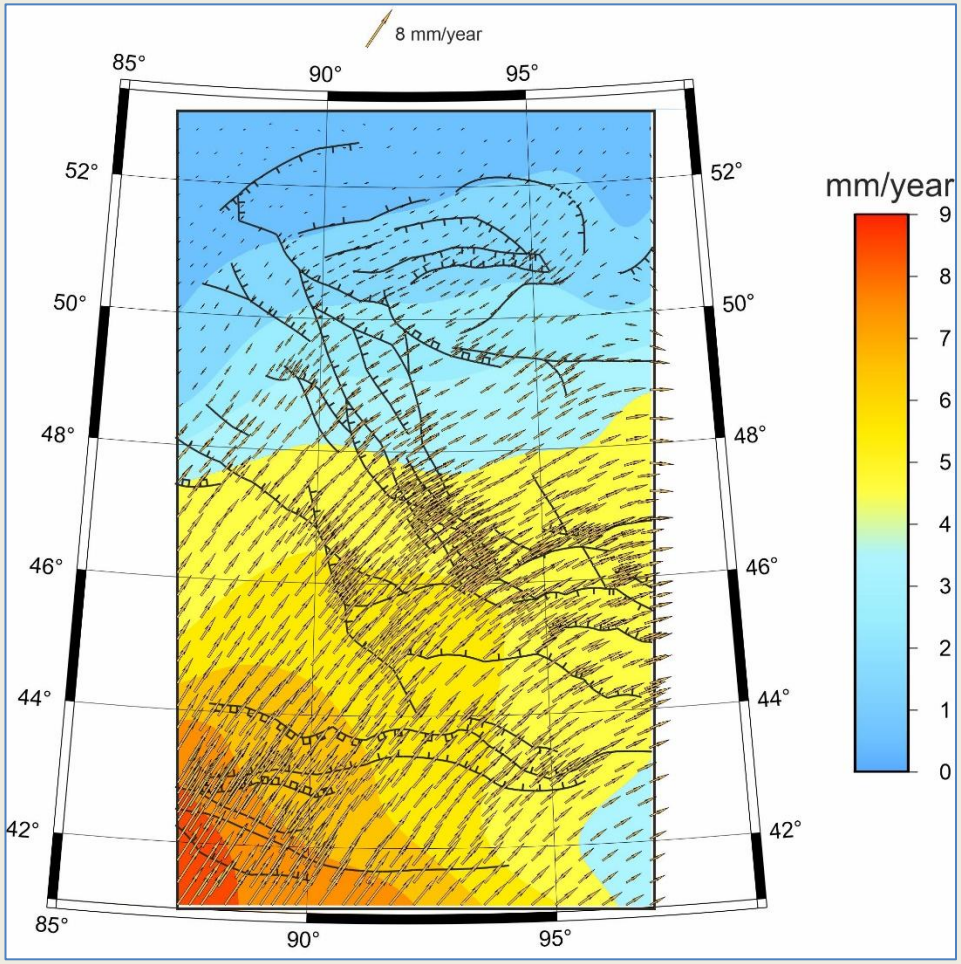

The PLATES program [Bird, Kong, 1994] was used. Inelastic deformations of the lithosphere model with inhomogeneities (faults) are simulated.

Model rates of deformation of the earth's crust of the Mongolian Altai

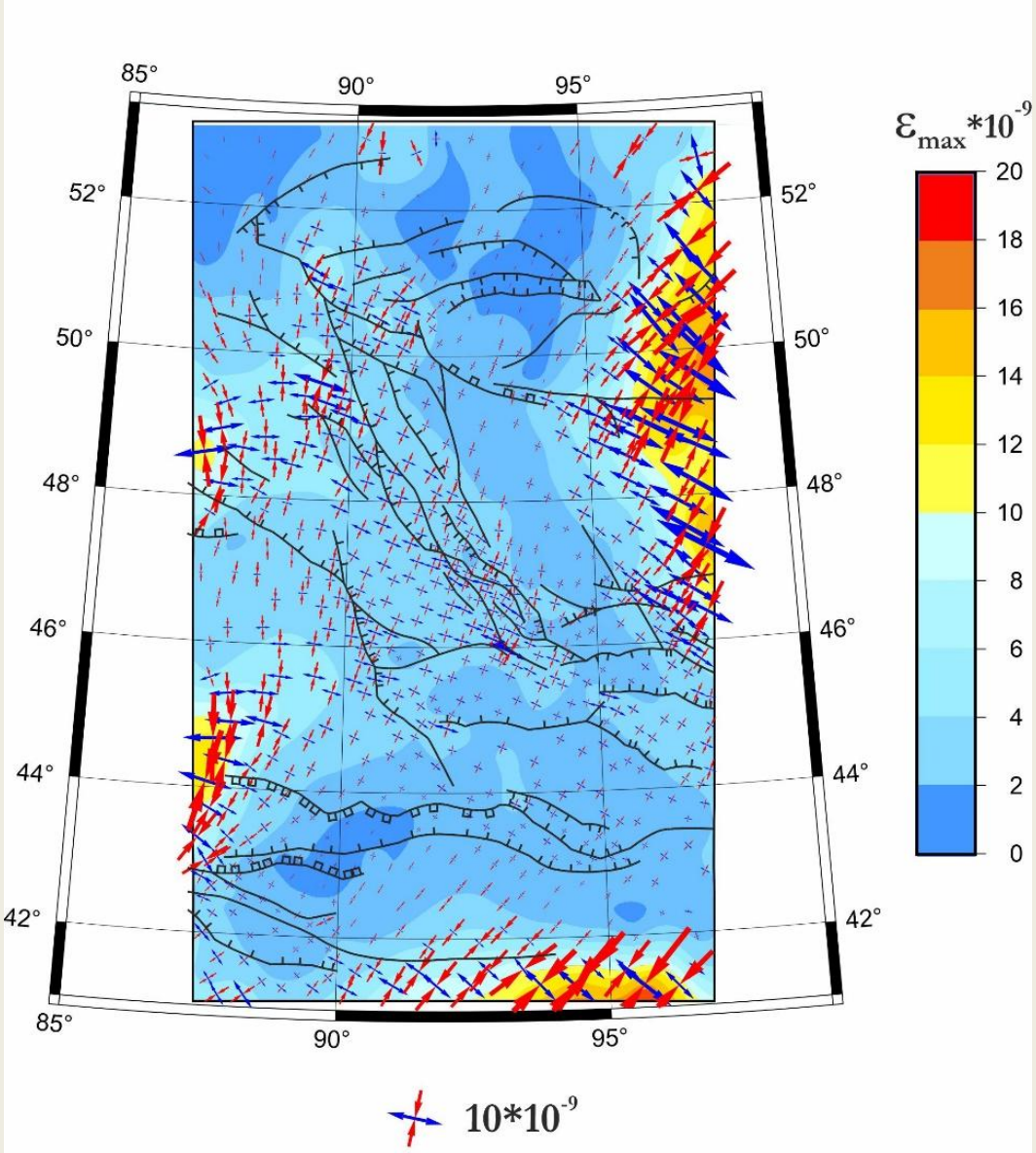

Model displacement rates along active faults of the Mongolian Altai and surrounding structures

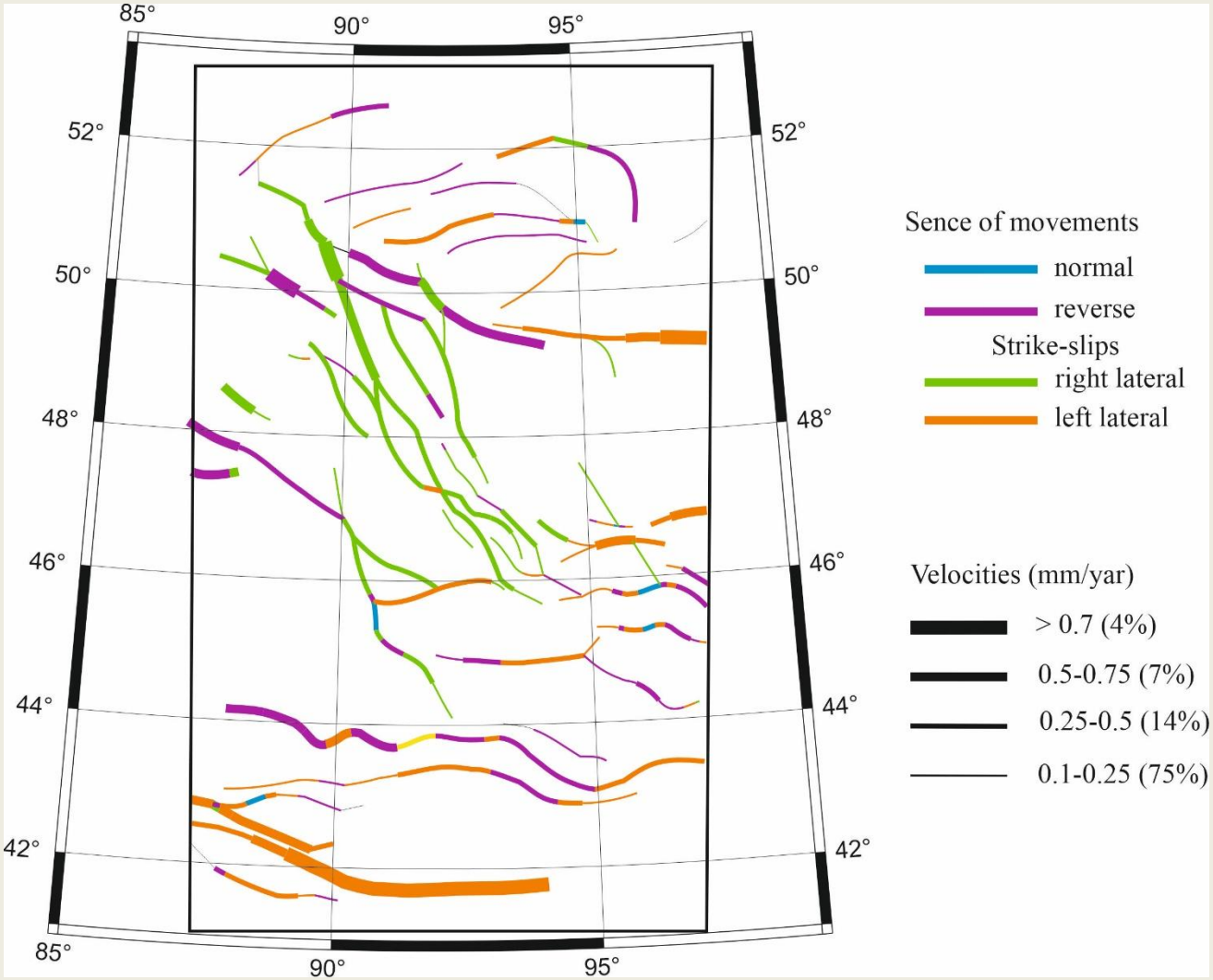

Velocities of displacements and rotations in fault zones of the Mongolian Altai and surrounding structures (summary of Gregory et al., 2018)

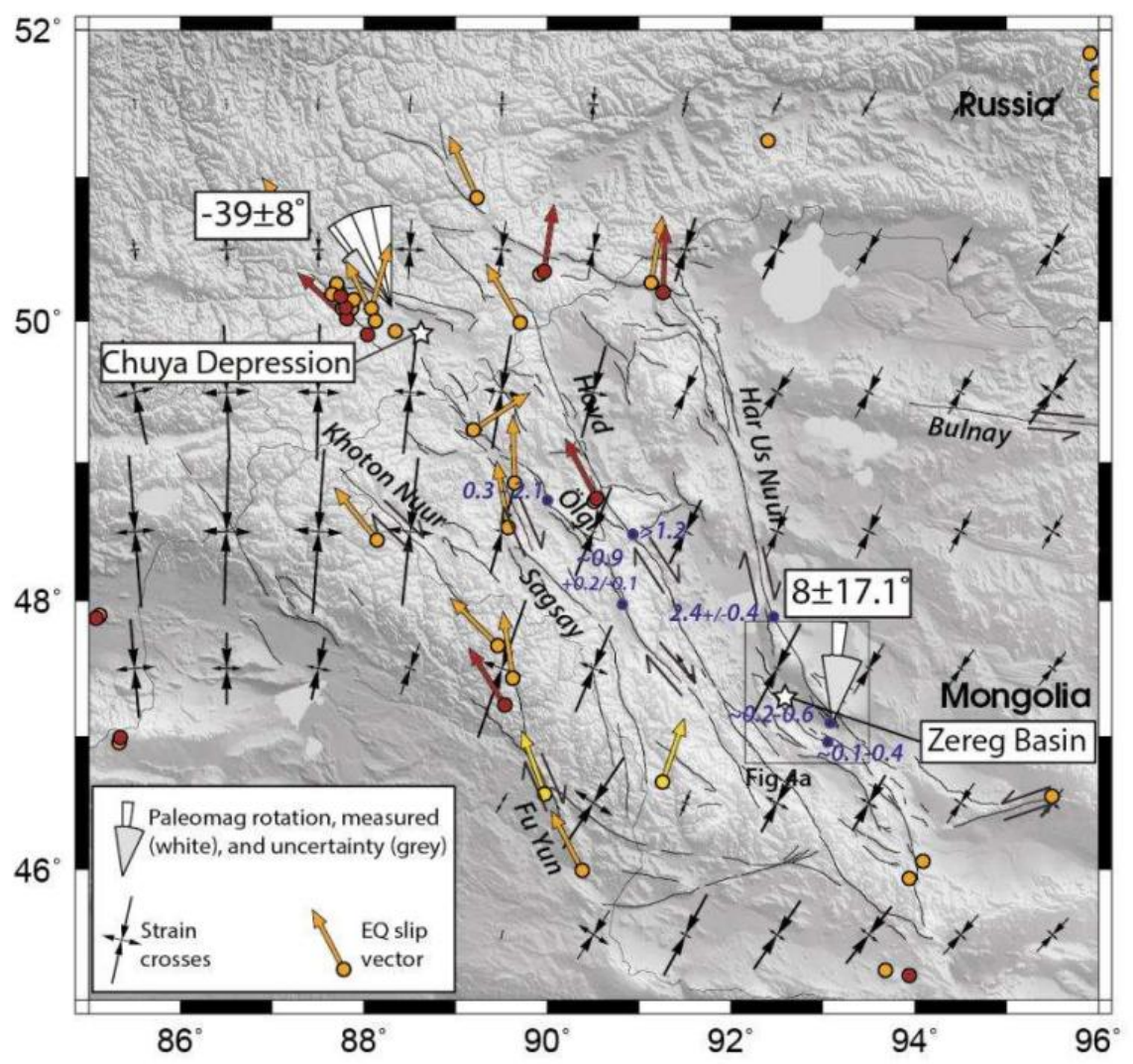

Data from Frankel et al. (2010); Gregory et al. (2014); Nissen et al. (2009a); Nissen et al. (2009b); Vassallo (2006); Thomas et al., 2002.

Conclusion

- The stress-strain state of the Mongolian Altai and surrounding structures in the late Cenozoic arose during compression due to the convergence of Hindustan and Eurasia. The predominant reconstructions of the stress state of the earth's crust based on geological-structural and seismological data are the stress tensors of compression and transpression, as well as strike-slip.
- MZ-KZ sedimentary cover of intermontane basins is deformed at the initial stage under conditions of sublatitudinal and NE compression with the formation of fold-and-thrust structures. There is a tendency for the direction of compression to change over time to NNE and submeridional and the manifestation of shear structures.
- In western Mongolia, structural control of the stress state of the earth's crust is carried out by fault zones of northwest and sublatitudinal strike.
- Modeling using the finite element method made it possible to reproduce the type of modern stress state and the directions of the main deformations on different structures and their sections.
- The model reproduces the kinematics and velocities of displacements along active faults, which can be used to assess seismic hazard in fault zones.


THANK YOU FOR ATTANTION!